water

MDPI

Article

What Controls the Flushing Efficiency and Particle Transport Pathways in a Tropical Estuary? Cochin Estuary, Southwest Coast of India

Sebin John [1,2], K.R. Muraleedharan [1,*], C. Revichandran [1], S. Abdul Azeez [1], G. Seena [1,2] and Pierre W. Cazenave [3]

1 CSIR-National Institute of Oceanography, Regional Centre, Kochi 682018, India; sebinjohn111@gmail.com (S.J.); revi@nio.org (C.R.); sabdulazeez44@gmail.com (S.A.A.); seena24.murali@gmail.com (G.S.)
2 Research Scholar, Bharathidasan University, Tiruchirappalli 620024, India
3 Plymouth Marine Laboratory, Plymouth PL1 3DH, UK; pica@pml.ac.uk
* Correspondence: muraleedharan@nio.org

Received: 3 December 2019; Accepted: 21 January 2020; Published: 23 March 2020

Abstract: Estuaries with poor flushing and longer residence time retain effluents and pollutants, ultimately resulting in eutrophication, a decline in biodiversity and, finally, deterioration of water quality. Cochin Estuary (CE), southwest coast of India, is under the threat of nutrient enrichment by the anthropogenic interventions and terrestrial inputs through land runoff. The present study used the FVCOM hydrodynamic model coupled with the Lagrangian particle module (passive) to estimate the residence time and to delineate site-specific transport pathways in the CE. The back and forth movements and residence time of particles was elucidated by using metrics such as path length, net displacement and tortuosity. Spatio-temporal patterns of the particle distribution in the CE showed a similar trend during monsoon and post-monsoon with an average residence time of 25 and 30 days, respectively. During the low river discharge period (pre-monsoon), flood-ebb velocities resulted in a minimum net transport of the water and longer residence time of 90 days compared to that of the high discharge period (monsoon). During the pre-monsoon, particle released at the southern upstream (station 15) traversed a path length of 350 km in 90 days before being flushed out through the Fortkochi inlet, where the axial distance was only 35 km. This indicates that the retention capacity of pollutants within the system is very high and can adversely affect the water quality of the ecosystem. However, path length (120 km) and residence time (7.5 days) of CE were considerably reduced during the high discharge period. Thus the reduced path length and the lower residence time can effectively transport the pollutants reaching the system, which will ultimately restore the healthy ecosystem. This is a pioneer attempt to estimate the flushing characteristics and residence time of the CE by integrating the hydrodynamics and Lagrangian particle tracking module of FVCOM. This information is vital for the sustainable management of sensitive ecosystems.

Keywords: Cochin Estuary; FVCOM; Lagrangian trajectory; residence time; freshwater influx

1. Introduction

The estuarine environment is one of the most exclusive productive systems on the Earth, supporting unique communities of species specially adapted for life in a highly changing environment. Many industries and human settlements in and around the estuaries are draining large amounts of effluent discharges [1]. Similarly, anthropogenic interventions create disturbances and pressure on the system that result in the eutrophication of water bodies and a decline in biodiversity. The self-purification capacity of the estuarine system strongly depends on its hydrodynamic conditions, such as tides,

currents and freshwater influx. Estuaries with poor flushing and longer residence time tend to retain nutrients within the system, leading to high primary productivity rates [2]. In contrast, well-flushed estuaries are more resilient to nutrient loading due to reduced residence time and greater exchange, with less impacted coastal waters. The rate of exchange is generally determined by three time scales, viz. flushing time, age of water, and residence time [3]. (1) Flushing time is the time required to replace the existing freshwater in the estuary at a rate equal to the river discharge. The flushing time characteristics can be computed in two ways viz. the classical approaches of the tidal prism and freshwater fraction methods. (2) Age of the estuarine water body represents the time taken for a dissolved or suspended material at any location to be transported from its source to its current location [4]. (3) Estuarine residence time can be defined as the average time interval the water parcel needs to cover its path through the estuary. It is a major driver of eutrophication and water quality [5], which results in the impairment of the ecological function of estuaries in terms of biodiversity, habitat quality, and trophic structure. The calculation of residence time for particles in natural reservoirs was described by Bolin and Rodhe [6], and the concept was further extended and modified for coastal sea applications [7,8].

About 70% of the chemical industries of Kerala state (India) are located in the Ernakulum district, dotted along the banks of the rivers Periyar and Chitrapuzha (Figure 1). The northern part of the CE (Angamali to Kochi region) is highly overwhelmed with >50 large and medium industries and 2500 small scale industries. This estuary receives high concentrations of industrial effluents of 104×10^3 m^3 per day and untreated domestic wastewater of about 0.26×10^3 m^3 per day [9]. Cumulative daily freshwater intake of the industries located in the Edayar to Eloor region is 1.8×10^5 m^3, and they discharge 75% of this intake water to the river as effluent water. The major types of these industries are fertilizers, pesticides, chemicals, and allied industries, petroleum refining and heavy metal processing, radioactive mineral processing, rubber processing units, animal bone processing units, battery manufacturers, acid manufacturers, pigment and latex producers. High concentrations of Fe, Mn, Zn, Cu, Cd, Pd, Cr, Co and Ni in the surficial sediments of the estuary were reported in the northern parts of the estuary [10–13]. On the other hand, houseboat tourism (604 houseboats, 308 private motorboats and 33 speed boats) discharges wastewater of 0.23 million litres per day and an unaccountable quantity of oil spillage that inversely affect the estuarine environment [14]. A recent study by Sruthy and Ramasamy [15] reported evidence of microplastics (96–496 particles m^{-2}) in the sediment, which not only has a direct impact on the aquatic environment and habitats but also set off cascade perturbations in the entire food web. Since large freshwater influxes contributed by prolonged monsoon enhance the complexity of residence time, it is very relevant to identify the retaining capacity of the CE. Thus, anthropogenic and terrestrial inputs adversely affect the health of the estuarine ecosystem, which needs immediate attention by addressing the transport process of the pollutants in detail.

Sustainable management of any ecosystem strongly depends on the dilution, dispersion and transport dynamics of the waste that is received from various point and non-point sources. Proper understanding of pollutant transport in the CE is very important because it holds 24th place in the critically polluted areas of India [16]. Nearly 1.6 million peoples [17] live on the banks of the CE in 38 local government bodies (3 municipalities and Cochin corporation) that spread across three districts (Ernakulum, Kottayam and Alappuzha). Domestic sewage from the urban areas of Alappuzha and Kochi is about 2550 million litres per day. Indiscriminate application of pesticides, industrial effluents and lack of adequate sanitation facilities during the closure period of the Thanneermukkom barrier aggravated the water pollution. According to Remani et al.(2010) [18], sewage waste will double (~428 million litres per day) from the present value (~227.2 million litres per day) by the year 2034, considering the projected population of Ernakulum, Alappuzha and Kottayam districts. Over the years, CE has been subjected to heavy eutrophication and this has resulted in the deterioration of the water quality, but a systematic approach to understanding the spatial and temporal variations of circulation and residence time is still lacking. Previous efforts focused on estimating the flushing characteristics of

the CE using the tidal prism method and flushing time by estuarine volume and freshwater fraction methods. These methods have limitations in systems like the CE, owing to the highly complex hydrodynamic conditions [19,20]. Field experiments to address the residence time are expensive and require vast human resources; hence, it is highly appropriate to use a 3D hydrodynamic model. The results provide an insight to understanding the deposition of sediments, debris, pollutants (physical characteristics), and thereby elucidate the origin, path and fate of the water parcel in time. This study offers one possible way to address the flushing efficiency of the CE in terms of residence time.

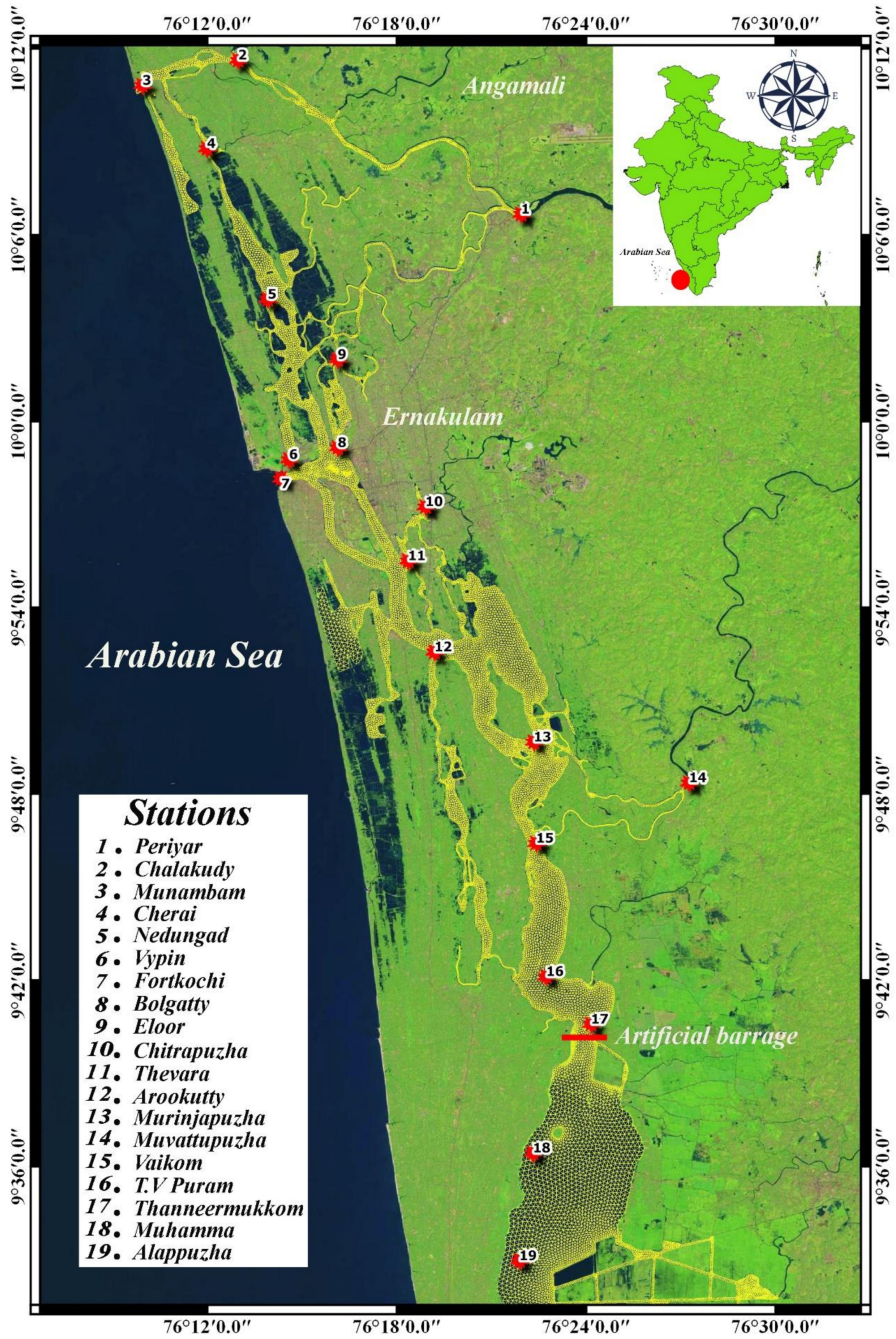

Figure 1. Cochin Estuary (CE) is situated in the state of Kerala (red filled circle in the in-site map), Southwest coast of India. This satellite (Landsat-8) image showed the model domain with the unstructured grid (yellow), and the major stations are numbered (1–19) on this map. An artificial barrage was constructed to prevent salt intrusion during the pre-monsoon period are marked by red line in this map.

2. Materials and Methods

The hydrodynamic condition of the CE was elucidated with the help of the Finite Volume Community Ocean Model (FVCOM, v. 4.1). It is an unstructured grid, finite-volume, free surface, three-dimensional primitive equation coastal ocean model that solves momentum, continuity, temperature, salinity, and density equations [21]. The CE is directly connected to the Arabian Sea through two inlets (Figure 1), one at Fortkochi (450 m wide, depth >15 m) and the other at Munambam (250 m wide, depth >7 m). The tide is mixed semidiurnal in nature, with a range of 1 m that progressively decreases upstream [22–24]. The CE is aligned parallel to the Arabian Sea over 96 km from Munambam to Alappuzha. The system receives a high amount of freshwater discharge (22×10^9 m^3/yr) annually from seven major rivers (Figure 2; Figure 3) with peak discharge during the summer monsoon [23]. Hence, the proper estimation of surface water elevation (m) at the ocean boundary, as well as at the confluence of each river to the model domain, are of prime importance to hydrodynamic modelling. Surface water elevations at each hour were calculated at the two open ocean boundaries using 25 tidal constituents. These tidal constituents were derived from the one-year tide data at Munambam and Fortkochi (Ocean/Open Boundaries) using the Tidal Analysis Software Kit 2000 developed at Proudman Oceanographic Laboratory in the United Kingdom. The daily river discharge data was applied to the model domain from the river gauge stations (sourced from the Central Water Commission—CWC, Government of India). The model domain consists of unstructured triangular grids with resolutions ranging from 10 to 600 m and contains 15,479 nodes and 22,520 elements (Figure 1). The uniform sigma-coordinate system was applied with 10 levels for vertical grid resolution (see Supplementary Figure S1). The base map was digitized using LISS-III and the corresponding grid was generated with Gmsh (version 2.5), developed by Geuzaine and Remacle (2009) [25]. The bathymetry data for the model was derived from digitizing the Inland Water Authority Plan Chart 2006 (IWAI, NW-3) using QGIS (see Supplementary Figure S2). The bottom roughness parameter was set to 0.035, with minimum value 0.015 for the model drag co-efficient and initial conditions provided by the simulation from the previous year, to produce an hourly output of three-dimensional currents, temperature, turbulent diffusivity, and 2D water level fluctuations. During the pre-monsoon period (January–April), the tidal propagation was obstructed due to the closure of the Thanneermukkom barrage to prevent salt intrusion towards the upper reaches of the CE. Hence the pre-monsoon simulations incorporated the feature of an artificial barrage in the model domain and it created the stagnant waterbodies at upper reaches of CE. FVCOM model simulations were performed for the period of 2009 to 2015 for validation with available seasonal hydrographic datasets.

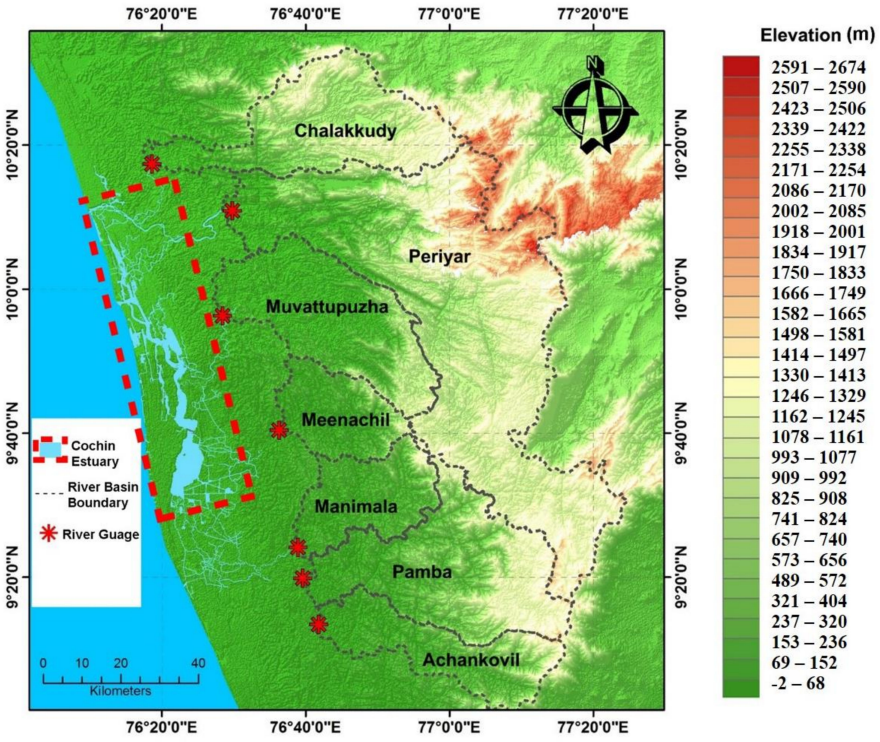

Figure 2. Study region (red box) encompassing the Digital Elevation Model map (Shuttle Radar Topography Mission, 90 m resolution) and Central Water Commission river gauge stations (red dots).

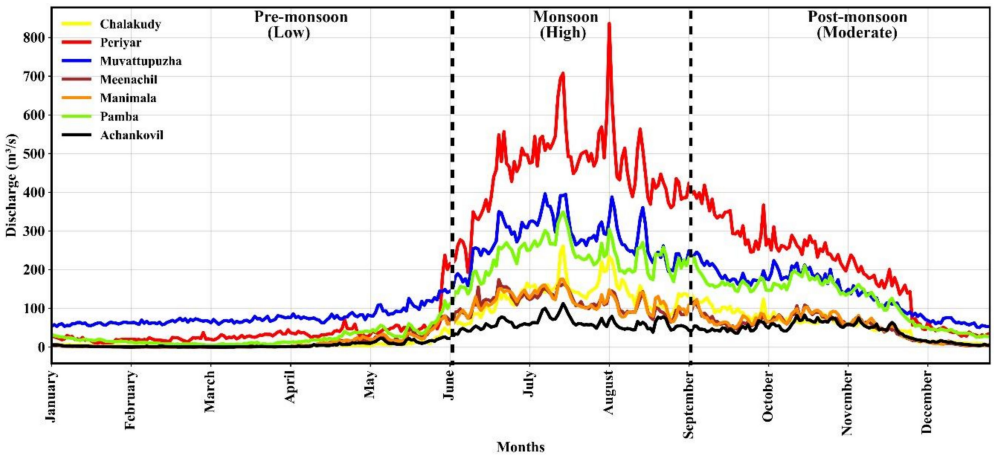

Figure 3. Daily climatological river discharges of the seven rivers at CE. Discharge data sourced from Central Water Commission, Government of India (2000–2016).

2.1. In-Situ Observations

One-month-long time-series observations (Table 1) of water levels and currents were conducted on the CE during low (22 February 2010–22 March 2010) and high river discharge periods (24 July 2010 12:00 a.m. to 21 August 2010 12:00 a.m.). Water levels were recorded from seven different locations (Figure 4) for 10-min intervals using a Seabird SBE-26 plus water level recorder, having an accuracy of 0.1% of full-scale (strain gauge pressure). Acoustic doppler current meters (Aanderaa RCM-9) were used to record speed (accuracy of ±0.15 cms^{-1}) and direction (accuracy of ±2°) for 10-min intervals from four stations (Figure 4). Daily surface salinity (0.4 m below surface) monitoring was carried out using an SBE 19 plus CTD (conductivity ± 0.001 S/m) at Vypin and Bolgatty (Figure 4), covering a period from 1 June 2013 to 31 May 2014 between 10:30 a.m. and 11:30 p.m. respectively (Table 1). Water samples (0.4 m below surface) were collected from four locations simultaneously at 11:00 a.m. on a daily

basis (Eloor, Arookutty, Thanneermukkom and Alappuzha) during the year 2014 by involving public participation, and samples were analysed in the laboratory using Eutech salinity probes. In addition to those observations, we also conducted an *in-situ* salinity profiling survey (Figure 4) in August 2013 (high discharge period) and March 2015 (low discharge period) using CTD-SBE19 Plus at 16 locations (from station 7 to 19). The corresponding data was extracted from the model output and validated with *in-situ* observations.

Table 1. Seasonal hydrographic data collected at different stations of CE during the period of 2010 to 2015.

In-Situ Observation Dates	Tide	Currents	Surface Salinity (0.4 m Below the Surface)	Salinity Profiles
22 February 2010–22 March 2010	3, 5, 7, 12, 15	3, 7 (surface and bottom), 17		
25 July 2010–21 August 2010	3, 4, 7, 12,15, 17	3, 7 (surface), 12, 17		
21 July 2013–25 December 2014			6, 8, 9, 12, 17, 19	
12–21 August 2013				Between 7 and 19
24–27 March 2015				Between 7 and 19

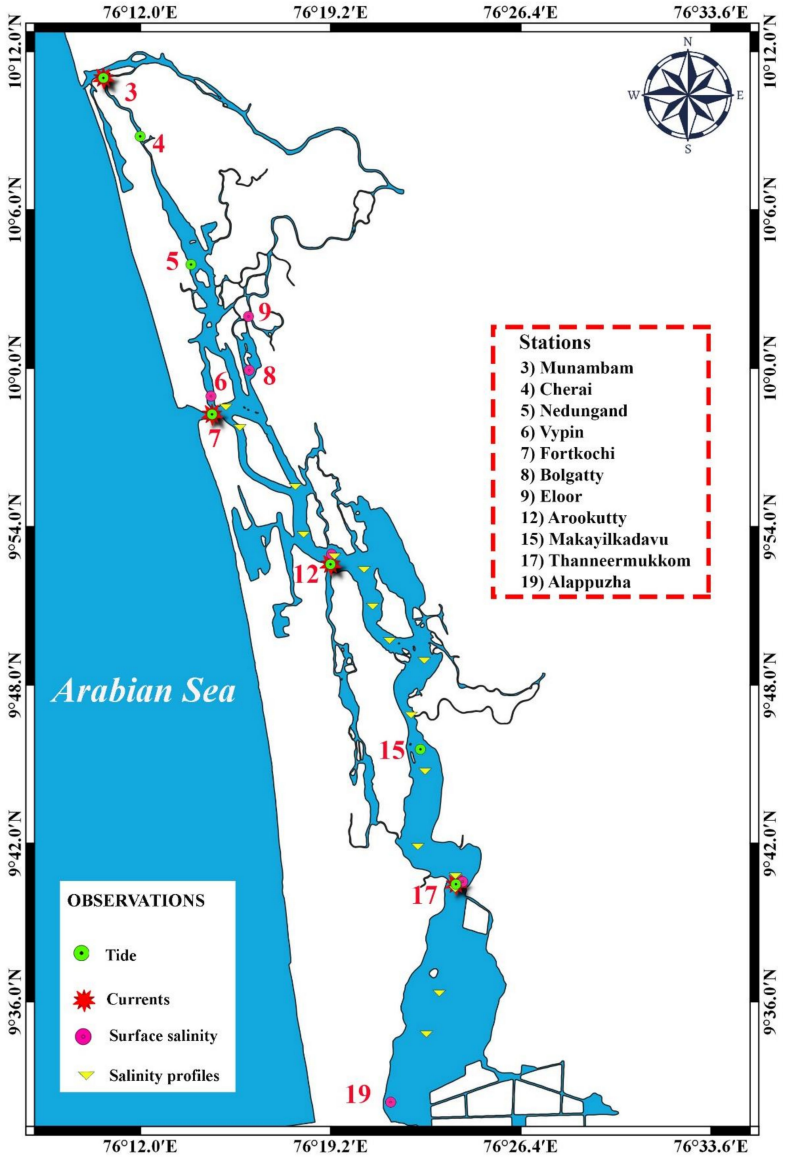

Figure 4. Sampling locations for model validations (tides, currents and salinity).

2.2. Validation of the Model

The reliability of the model was expressed using the Taylor diagram (plotrix package in R) and the index of agreement (d). Willmott (1981) [26] proposed a new approach in the model skill index of agreement (d), which can be defined as

$$d = 1 - \frac{\sum_{i=1}^{N} (P_i - O_i)^2}{\sum_{i=1}^{N} \left(\left| P_i - \overline{O} \right| \left| O_i - \overline{O} \right| \right)^2} \quad (1)$$

where P and O represent the predicted model and observed values, respectively. $\overline{O}$ is time mean of O, and N is the size of the data set. Perfect agreement between model results and observations yields a skill value of one, and complete disagreement gives a skill value of zero.

2.2.1. Tide

The assessment of the model performance begins with analysing the tidal variations in surface water elevations with respect to in-situ measurements. The spring–neap variability of the CE and associated water level changes were able to be predicted precisely using the FVCOM model (refer to Supplementary Figures S3 and S4). The model performance was assessed qualitatively using an agreement of index and correlation. The surface water elevation at all stations was well captured with an average agreement of index of 0.96 and a correlation coefficient of 0.92 (Table 2). The maximum amplitude was noticed in Fortkochi (0.63 m in pre-monsoon), followed by Munambam (0.54 m in pre-monsoon) in the northern arm. The tidal dampening was high in the southern arm (stations 7–17) compared to the northern arm (stations 3–7). This can be attributed to the frictional dissipation and partly due to the presence of shallow and wide water bodies in the southern upstream. Among these locations, Fortkochi and Munambam have the best fit to the observed value, with an agreement of index and correlation coefficient of 0.99. Most of the stations exhibited ≥90% of correlation during pre-monsoon and monsoon except at Thanneermukkom (station 17), where the index of agreement was 0.86 and the correlation coefficient was 0.75.

Table 2. The index values and correlations of the predicted/simulated time series surface water elevations at seven locations in CE during pre-monsoon (2010) and monsoon (2010).

Stations	Index of Agreement		Correlation Coefficient	
	Pre-Monsoon	Monsoon	Pre-Monsoon	Monsoon
Munambam	0.99	0.99	0.99	0.99
Cherai	NM	0.95	NM	0.98
Nedungad	0.94	NM	0.94	NM
Fortkochi	0.98	0.99	0.97	0.99
Arookutty	0.95	0.98	0.93	0.97
Makayilkadavu	0.96	0.91	0.94	0.85
Thanneermukkom	NM	0.86	NM	0.75

NM = no measurements.

A Taylor diagram provides a graphical summary of how accurately simulated the surface water elevation is to the observation. In Figure 5, the similarity between the observation and modelled elevation were quantified in terms of correlation, centered root mean square differences and the amplitude variations. Simulated elevations that agreed well with observations lie nearest to the "observed" on the x-axis. These predicted elevations at seven locations showed good correlation and low RMS errors during both the seasons. However, the predicted elevations during pre-monsoon are comparatively close to the observed point on the x-axis than that of monsoon. The lowest correlation was observed at the stations Thanneermukkom (station 17) and Makayikadavu (station 15), which are located above the upstream regions of the CE.

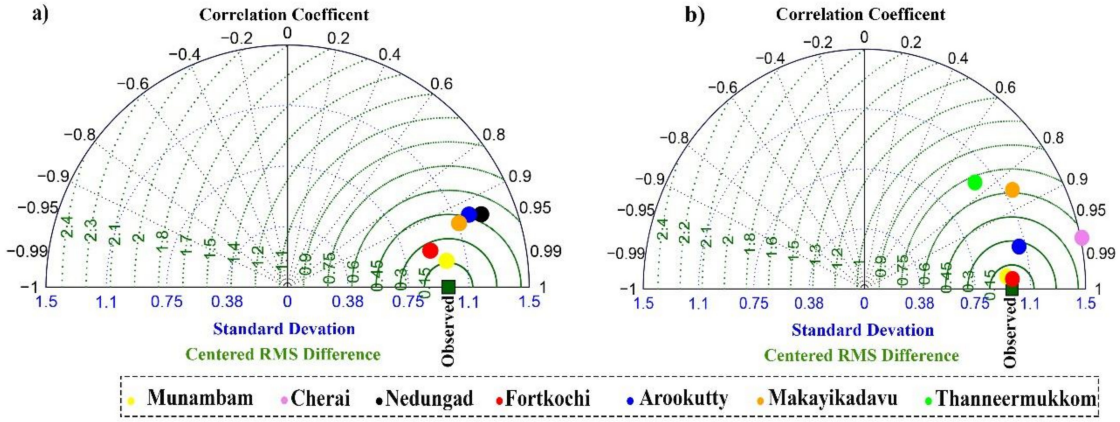

Figure 5. Normalized Taylor diagram for the statistical significance of the surface water elevation of the model during the (**a**) pre-monsoon (2010) and (**b**) monsoon (2010).

2.2.2. Currents

Currents in the CE are dominated by the tidal signals and the model was able to capture the diurnal inequality and spring–neap variability. Time series of along and across-channel velocities are shown in Supplementary Figures S5 and S6. The phase of the along and across-channel velocities of the model is exactly similar to that of the observed ones. The maximum flow velocity noticed in Fortkochi and Munambam was 1 and 0.7 m/s, respectively (Supplementary Figures S7 and S8). A comparison between the model and observed velocities (along and across-channel velocities) at four stations showed a good agreement of index for the predicted velocities with an average of 0.80 and the correlation of 0.78 (Figures 6 and 7, Table 3) during the pre-monsoon and monsoon. Bi-directional flow noticed at the Fortkochi inlet during the flood period (the surface layer flows towards the sea while the bottom layer flows to the lake) was captured by the model, where the index of agreement with the observed data at surface and bottom was 0.81 and 0.76, respectively (Table 3). Majority of the stations exhibit ≥70% of correlation in velocity during pre-monsoon and monsoon, except at Thanneermukkom. During pre-monsoon, the Thanneermukkom region experiences low correlation and index of agreement (0.6) with minimum flow velocity (<0.1 m/s) due to the closure of the Thanneermukkom barrage (Supplementary Figure S8b).

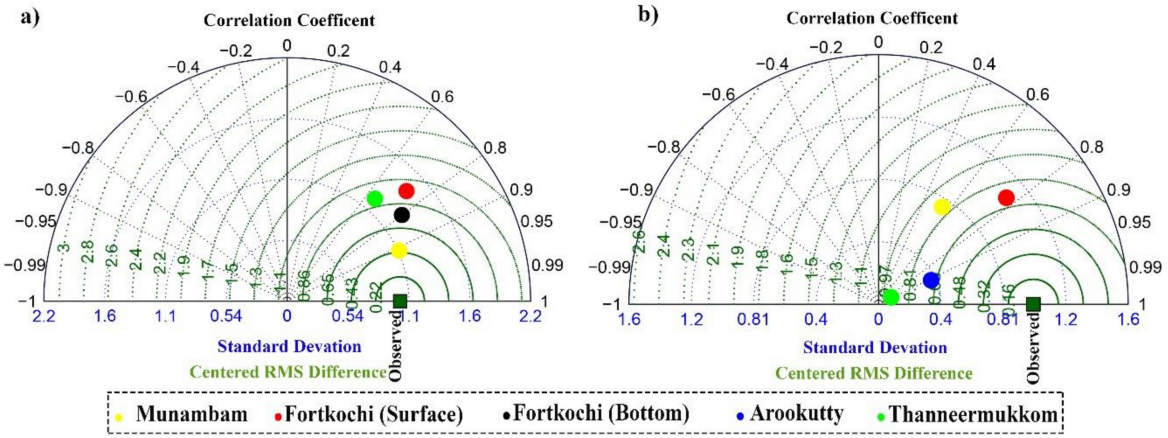

Figure 6. Normalized Taylor diagram for the statistical significance of along-channel velocity of the model during the (**a**) pre-monsoon (2010) and (**b**) monsoon (2010).

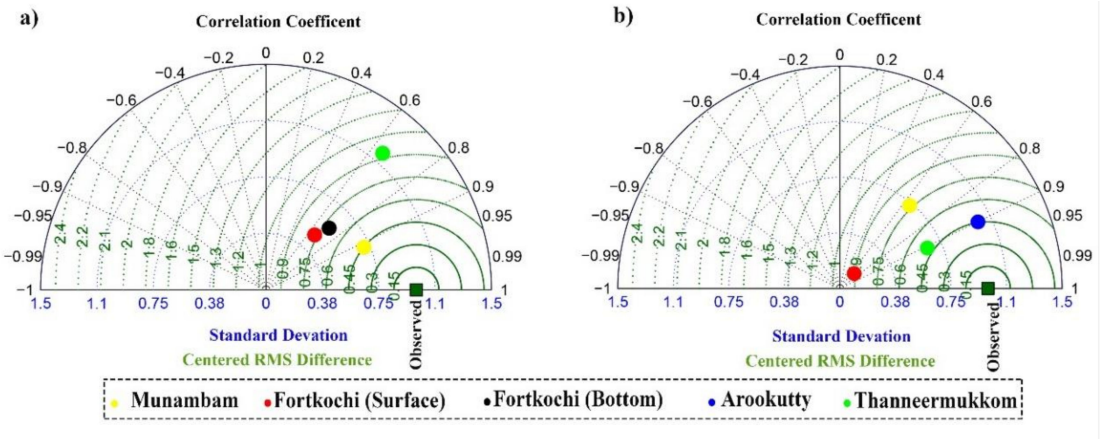

Figure 7. Normalized Taylor diagram for the statistical significance of across-channel velocity of the model during the (**a**) pre-monsoon (2010) and (**b**) monsoon (2010).

Table 3. Index values for the model and correlations of the time series currents (U and V components) at four locations in CE during pre-monsoon (2010) and monsoon (2010).

Stations	Velocity Components	Index of Agreement		Correlation Coefficient	
		Pre-Monsoon	Monsoon	Pre-Monsoon	Monsoon
Munambam	along	0.93	0.71	0.92	0.62
	across	0.84	0.81	0.92	0.64
Fortkochi (Surface)	along	0.76	0.87	0.74	0.77
	across	0.69	0.70	0.67	0.69
Fortkochi (Bottom)	along	0.81	NM	0.80	NM
	across	0.76	NM	0.72	NM
Arookutty	along	NM	0.94	NM	0.91
	across	NM	0.95	NM	0.90
Thanneermukkom	along	0.60	0.86	0.61	0.91
	across	0.61	0.80	0.62	0.87

NM = no measurements.

2.2.3. Salinity

Salinity distributions reflect the combined results of all processes, including density and gravitational circulations. During the simulation period, the FVCOM model was able to capture seasonal variation of the surface salinity (0.4 m depth) pattern with respect to the freshwater influx (Supplementary Figure S7). The large longitudinal salinity gradients were noticed and ranged from 0 psu (Eloor, Arookutty, Thanneermukkom and Alappuzha) to 35 psu (Vypin and Bolgatty). The Taylor diagram drawn for six locations showed (Figure 8 and Table 4) an average value of correlation of about 0.87 and the index of the agreement as 0.9 during 2013 to 2014. The majority of the stations showed similarity to the observed salinity in the normalized Taylor diagram. However, the maximum RMSE was at Eloor with correlation of 0.8, while the stations at Vypin and Alappuzha were underestimated in the standard deviation for the model. The vertical salinity section (Figure 9) from the model was compared with observed salinity in the southern estuary. During the monsoon, stratification was observed up to 12 km from the Fortkochi inlet and the remaining regions were fully occupied by freshwater, which is well matched with the model simulation (Figure 9a,b). In the pre-monsoon months, salinity intrusion was noticed up to 47 km (Thanneermukkom barrage). This barrage prevented salinity intrusion further to the southern part. The model also picked up salinity stratification to the upstream region during this period (Figure 10a,b).

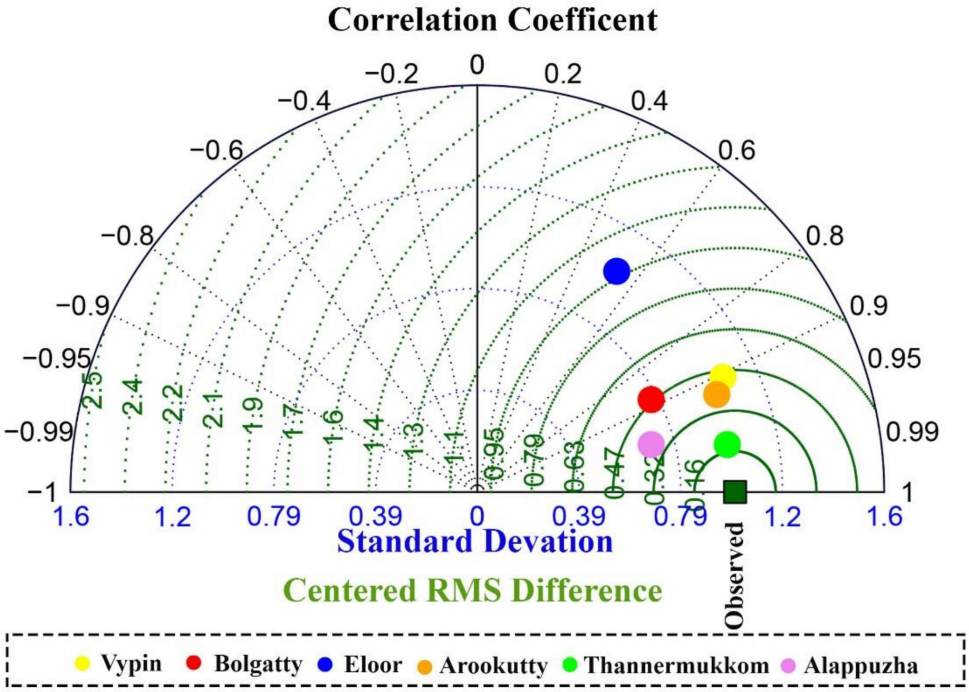

Figure 8. Normalized Taylor diagram for the statistical significance of surface salinity at 6 locations from 2013 to 2014.

Table 4. Index values and correlations of the predicted/simulated daily surface salinity at six locations in CE from 2013 to 2014.

Stations	Index of Agreement	Correlation Coefficient
Vypin	0.94	0.91
Bolgatty	0.94	0.88
Eloor	0.70	0.53
Arookutty	0.96	0.98
Alappuzha	0.88	0.96

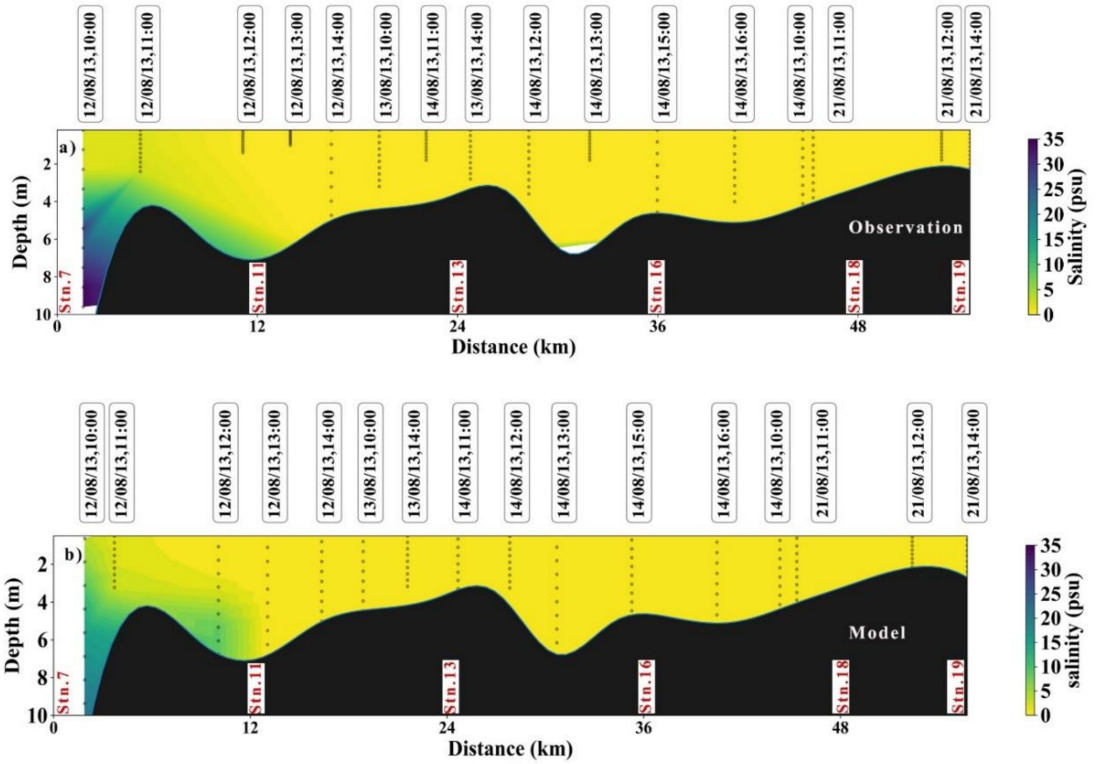

Figure 9. Validation of vertical salinity at CE during the period of 12–21 August 2013 (**a**) observation and (**b**) model.

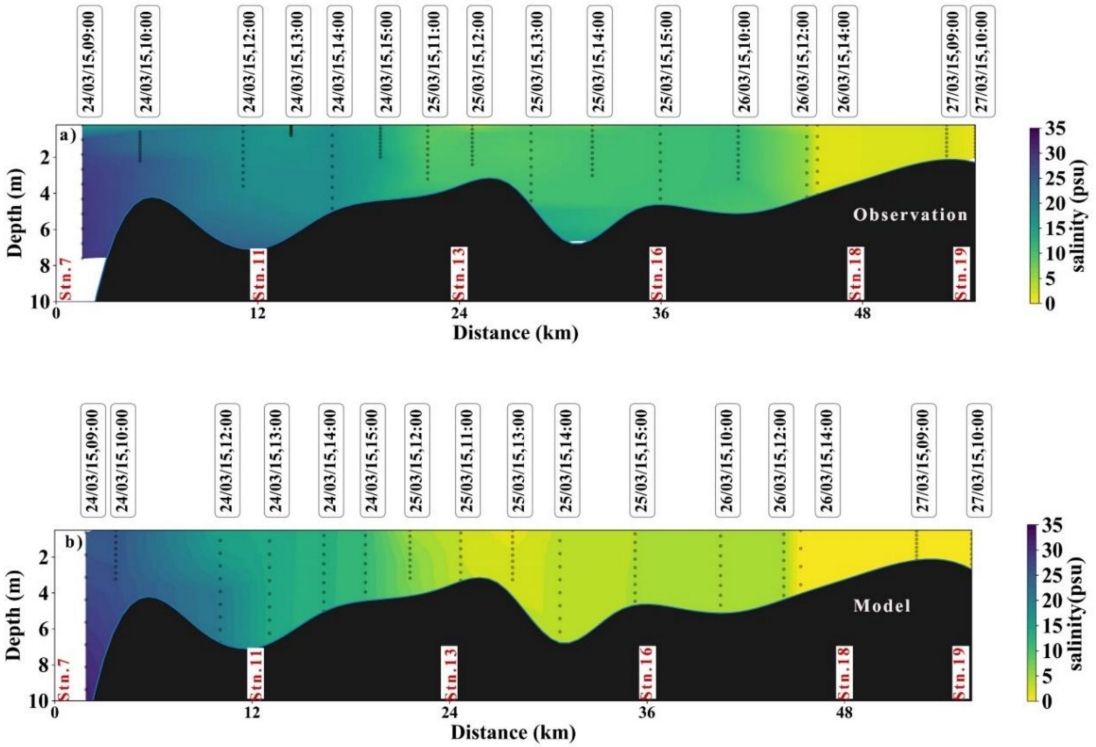

Figure 10. Validation of vertical salinity at CE during the period of 24–27 March 2015 (**a**) observation and (**b**) model.

2.3. Lagrangian Particle Tracking Model

The Lagrangian particle-tracking technique has been widely used to estimate the transport time scales in a number of water bodies with varying complex dynamics and geometries. This technique was used to study larval transport in the Gulf of Maine [27,28] and applied in the Great Lakes [29]. In the present study, FVCOM coupled with the Lagrangian particle module was used to estimate the residence time and the site-specific transport trajectory of the CE. Model simulations were performed for three distinct seasons, pre-monsoon (January–March), monsoon (June–August) and post-monsoon (October-December), according to the river discharge (Figure 4). For model simulation, we used the climatological river discharge of seven rivers, which was generated from daily river discharge data sets spanning from 2000 to 2016, obtained from the Central Water Commission (CWC), Government of India. We confined our discussion only to major scenarios such as high discharge (monsoon) and low discharge periods (pre-monsoon; closure period of the barrage at Thanneermukkom). In order to understand the water transport trajectories, 2584 particles were evenly distributed in the CE with a spatial resolution 300 m. These particles were defined as neutrally buoyant, passive in nature and released at the surface layer (sigma layer = 1), which was tracked until they flushed out from the system. As the objective of this study is the qualitative and quantitative estimation of flushing characteristics and residence time of the estuarine system, the transient waters were not considered. The distribution of these particles were analysed for 60–90 days during each season and their positions were recorded at 1-hour intervals. The flushing through both inlets in the CE was quantified by the percentage of particles transported out of the system. The residence time (days) for each particle was calculated as the time period at which the particles resided in the CE. The mean residence time of the estuary was estimated by the e-folding time, which is the time taken to decrease the particles to 1/e (37%) from the initial particle numbers. This can be calculated by applying ensemble averaging of the individual particle's residence time in the domain after release [30].

$$T_{re} = \frac{1}{R}\frac{1}{N}\sum_{j-1}^{R}\sum_{i=1}^{N}(t_r)_{ij} \tag{2}$$

where T_{re} is the mean residence time based on the ensemble averaging, R is the total number of release, N is the total number of particles, and $(t_r)_{ij}$ is the residence time for the ith particle in jth release.

The back and forth movement of the particle released in the model domain can be estimated using metrics such as the path length, net displacement and tortuosity or relative meandering of the particle path. Tortuosity (τ) can be described as the ratio between the net displacement and path length that is subtracted from unity, such that a straight line of transport would have a value of 0 and a looped transport would have a value of 1.

$$\tau = 1 - \frac{d}{L} \tag{3}$$

The average path length (L) is calculated as the average of the total absolute distance travelled by a particle at each time step in all of the releases and given by

$$L = \frac{1}{R}\sum_{j=1}^{R}\sum_{i-1}^{m}\sqrt{\left(x_j^{i+1} - x_j^i\right)^2 + \left(y_j^{i+1} - y\right)^2} \tag{4}$$

where L is the average path length, m is the total number of time steps; x and y are the coordinates of a particle at a given time step.

To elucidate the major dynamics that control the flushing efficiency of the CE, we conducted two types of control run viz. Case 1: river **ON** and tide **OFF** condition and Case 2: river **OFF** and tide **ON** condition. In both cases, the trajectory of the released particles was identified to estimate residence time, path length, net displacement and tortuosity.

3. Results and Discussion

3.1. Spatial Distribution of the Particles during the Monsoon Period

Uniformly distributed particles (first time step—100%) and its temporal evolution according to the prevailing dynamics during the summer monsoon period are given in Figures 11 and 12. Fifty percentage of the particles were quickly flushed out (Figure 11) from the system (fast flushing phase); thereafter, particle trajectory becomes steady (slow flushing phase). Particles left the CE within the e-folding time; this revealed that the majority (90% of the e-fold time) of the particles were flushed through the Fortkochi inlet (station 7) and the remaining through the Munambam inlet (station 3). Particles residing at a radial distance of 8 km from the both inlets were completely flushed out within one day. The region between station 3 and 12 (Figure 12b) showed a residence time of 5 days except at Nedungad (station 5). This region exhibited a stagnant nature during the initial 20 days. Due to the recurring tidal excursion, the particles in the region moved south (station 3) and were flushed out within 5 days. This region (station 5) has been identified as a null zone by Ramamirtham and Muthusamy (1986) [31] and Balachandran et al. (2005) [13], which is well established with our studies. The fast flushing phase (50% of initial particles flushed out from the system) of the CE is about 16 days. Towards the southern part of the CE, a navigational channel is maintained at the western bank and hence faster movement was noticed compared with the eastern bank. The faster movements of the particles were noticed at station 13 (residence time—6 days) compared to the station 17 (residence time—17 days), which are mainly attributed to the immense discharge from the Muvattupuzha river (station 14). The average residence time of the CE in the monsoon period is 25 days, in which 67% of the initial particles were flushed out from the domain.

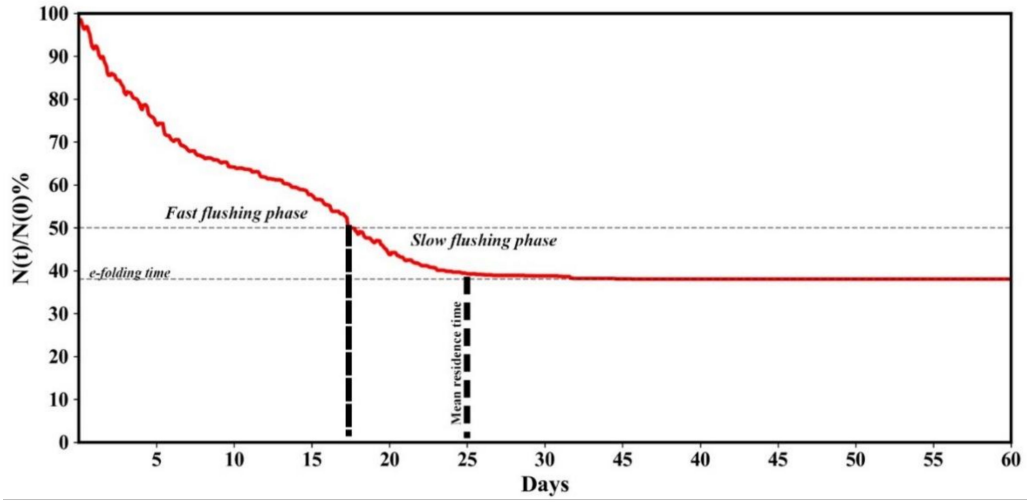

Figure 11. The residence time of CE during the monsoon season was calculated with a resolution of 300 m. A total of 2584 particles were realised over the model domain. N (0) is the initial number of particles in the domain and N (t) is the number of particles at time t. The percentage of particles initially reduced from 100% to 50% in the model domain is considered as the fast flushing phase, followed by a slow flushing phase.

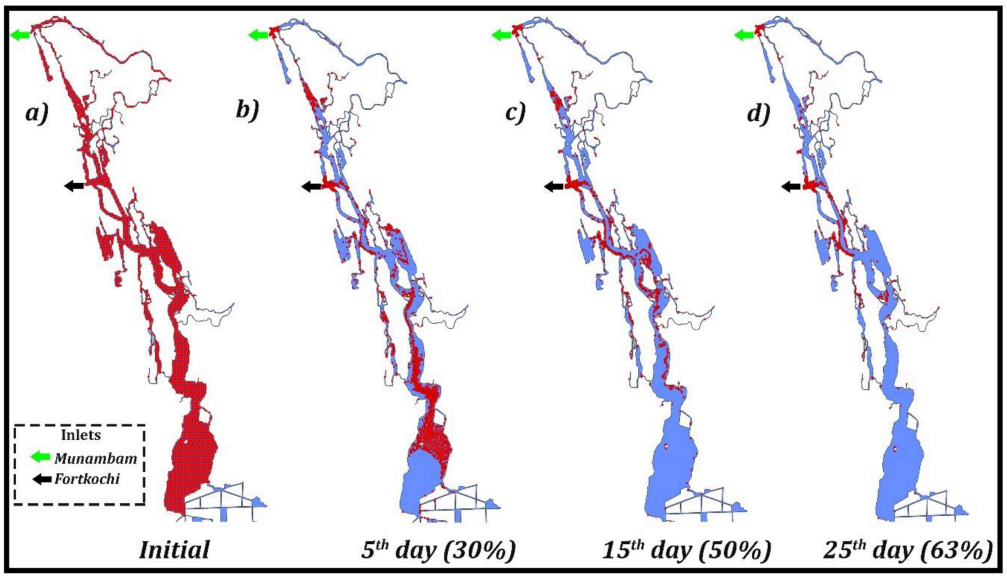

Figure 12. Spatial distribution of particles after the initial period (**a**), with 30% (**b**), 50% (**c**) and 63% (**d**) of the particles flushed out from the model domain with varying climatological freshwater discharge at the upstream boundaries during the summer monsoon.

Tortuosity gives an idea about the meandering path of the water parcel travelled by the effect of freshwater discharge and tidal activity. Tortuosity >0.6 implies that the average path length is approximately 2.5 times larger than the actual distance [30]. The minimum tortuosity of 0.3 was noticed at stations 2 and 3 (Figure 13c) and maximum (>0.8) at station 5. Particles released at station 17 took 17. 5 days to flushed out from the CE, by which it travelled a path length of 264 km (an actual axial distance of 48 km) under high discharge and tidal dynamics (Figure 13a,b).

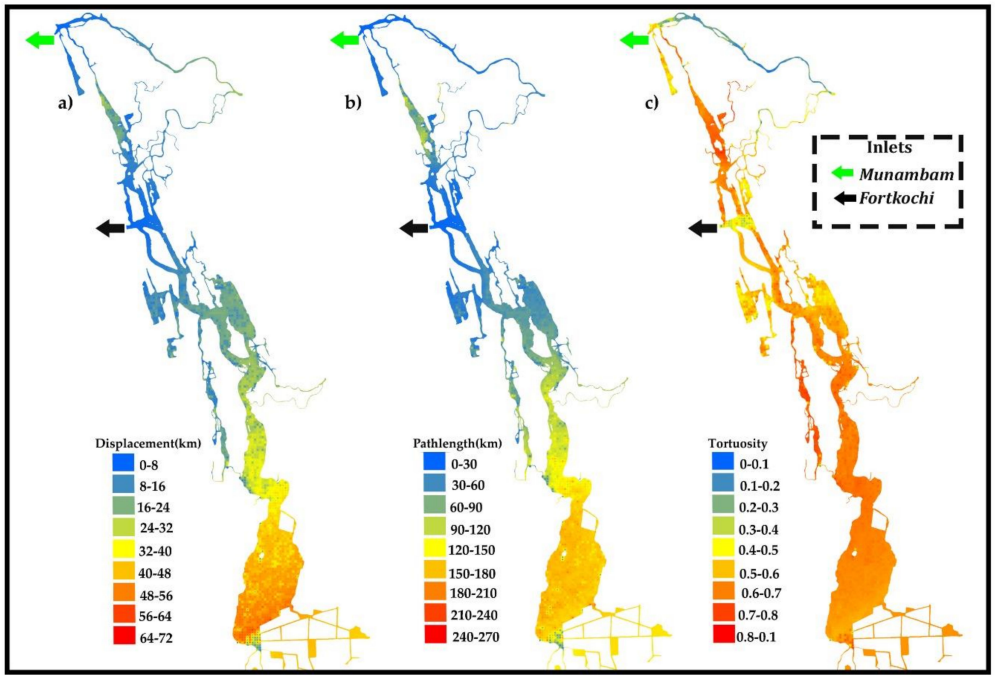

Figure 13. Displacement (**a**), path length (**b**) and tortuosity (**c**) of the CE during the summer monsoon.

3.2. Spatial Distribution of the Particles during the Pre-Monsoon Period (Barrage Closure Period at Thanneermukkom)

The particles movement was negligible at the south of the Thanneermukkom barrage (station 17) due to the closure of the barrage during this period. Low river discharge and overwhelming tidal dynamics significantly altered the flushing dynamics of the CE. Only 30% of the particles released in the CE were flushed out from the system (Figures 14 and 15). Particles at 8 km radial distance from both inlets were completely flushed out within one day, whereas the region between station 3 and 12 (Figure 15c) took 20 days for complete flushing except for a small region at station 5. However, these particles exhibited an oscillating nature within a limited distance upstream and downstream of the estuary depending upon the tidal phase. The artificial barrage at station 17 practically cut off the freshwater supply from the southern rivers Achankovil, Pampa, Meenachil and Manimala, consequently limiting particle displacement. The distinct lateral variation in the speed of the particles (eastern and western banks of the southern CE) could be attributed to the deep and shallow regions. The results showed that downstream transport of particles was much faster along the western bank, where the channel is comparatively deeper. Particles in the north of the artificial barrage (station 17) were more or less stagnant, presumably due to the prevailing standing waves. During the pre-monsoon, particles at station 15 traversed 350 km (Figure 16) in 90 days (residence time) before being flushed out through the Fortkochi inlet, whereas during the monsoon, the particles were flushed out within 17 days. Longer residence time noticed during the pre-monsoon is conducive for pollutant retention and the eventual degradation of the ecosystem.

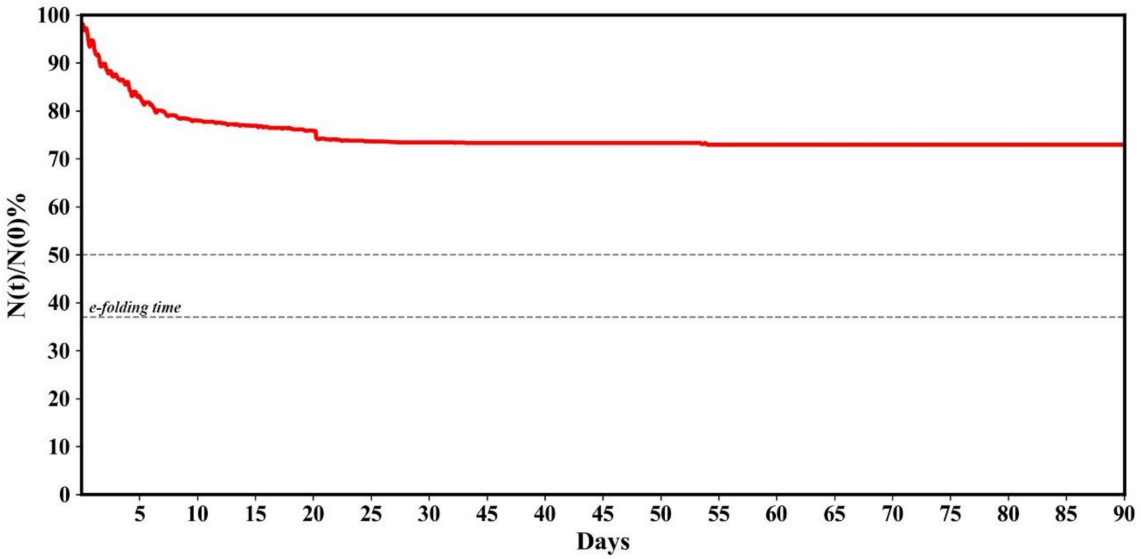

Figure 14. The residence time of CE during the pre-monsoon season was calculated with a resolution of 300 m. A total of 2584 particles were realised over the model domain. N (0) is the initial number of particles in the domain and N (t) is the number of particles at time *t*. Fast and slow flushing phases were not experienced in the pre-monsoon simulation.

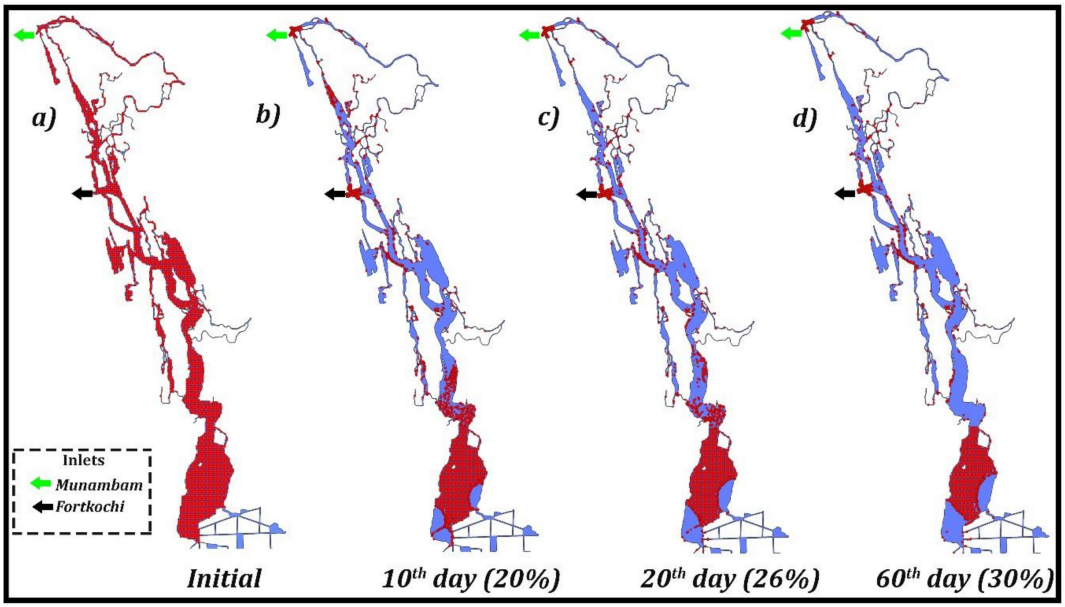

Figure 15. Spatial distribution of particles after the initial period (**a**), with 20% (**b**), 26% (**c**) and 30% (**d**) of the particles flushed out from the model domain with varying climatological freshwater discharge at the upstream boundaries during the pre-monsoon.

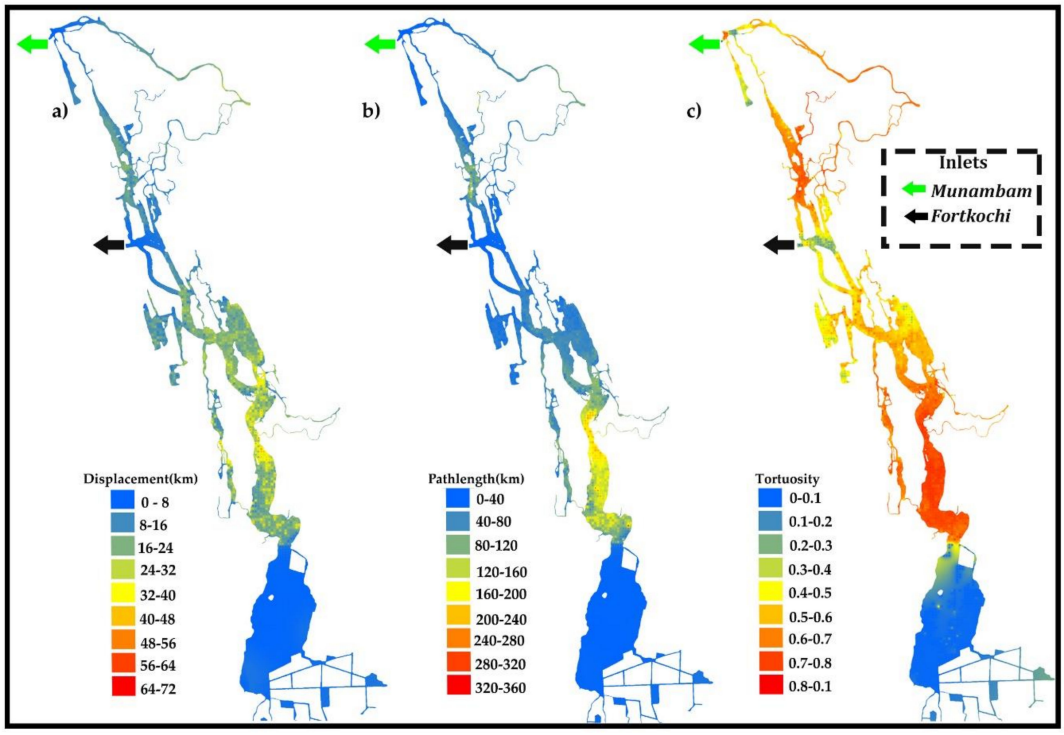

Figure 16. Displacement (**a**), path length (**b**) and tortuosity (**c**) of the CE during pre-monsoon.

3.3. Controlling Factors Determining the Flushing Characteristics of the CE

Case 1: Particles Released in the Model Domain with River ***ON*** *and Tide* ***OFF*** *Condition*

The estuarine region showed a unidirectional flow so that particles near to the inlet flushed out first and farthest within 22 days (Figure 17), which was 3 days earlier than the actual monsoon simulation. The back and forth movement of these particles was not evident, which corresponds to the same path length and net displacement of the particles and hence minimum tortuosity for the river ON and tide OFF simulation (Figure 18). The maximum path length of 70 km (Case 1) was noticed in

the southern upstream of the CE, which was twofold lower than path length in the actual monsoon simulation (160 km). This experiment confirmed that the particles were flushed with the least path length and comparable residence time to that noticed during the monsoon simulation.

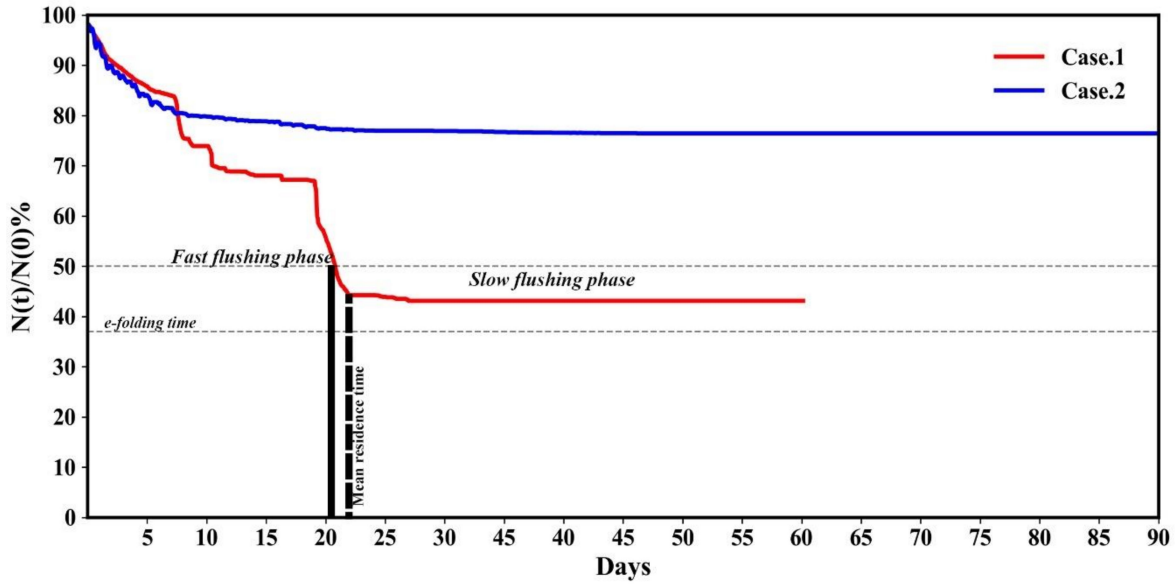

Figure 17. The residence time of CE is shown during the control run experiments of Case 1 (tide OFF and river ON) and Case 2 (tide ON and river OFF). Red and blue lines indicate the residence time patterns of CE in Case 1 and Case 2, respectively. N (0) is the initial number of particles in the domain and N (t) is the number of particles at time *t*.

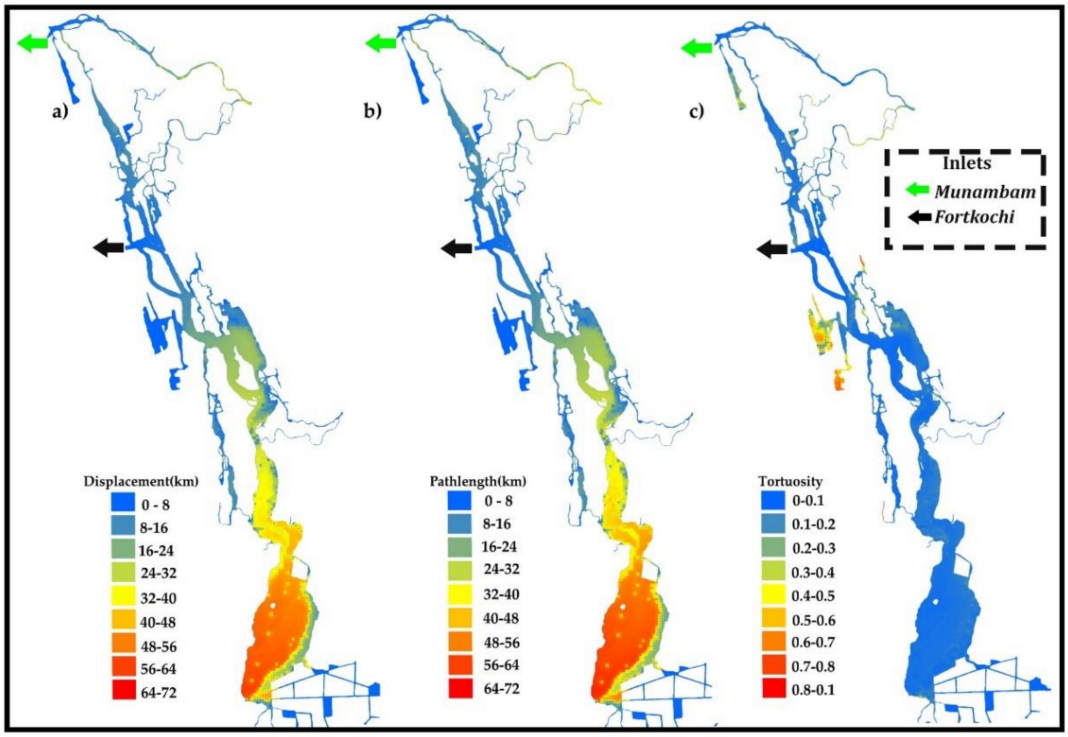

Figure 18. Displacement (**a**), path length (**b**) and tortuosity (**c**) of the CE during the control run simulation with Case 1 (river ON and tide OFF condition).

Case 2: Particles Released in the Model Domain with River ***OFF*** *and Tide* ***ON*** *Condition*

The average residence time of this simulation was almost comparable to that of the pre-monsoon simulation (90 days), where <30% of the particles were flushed from the system (Figure 17). A strong back and forth movement of these particles was noticed with the larger path length and high tortuosity in the river OFF and tide ON simulation (Figure 19). The flushing efficiency of CE was significantly reduced during the actual pre-monsoon simulation, which was clearly reproduced in the Case 2 simulation. This experiment also confirmed the least flushing nature of the CE with larger path length, high tortuosity and longer residence time, and almost corresponds to the pre-monsoon simulation.

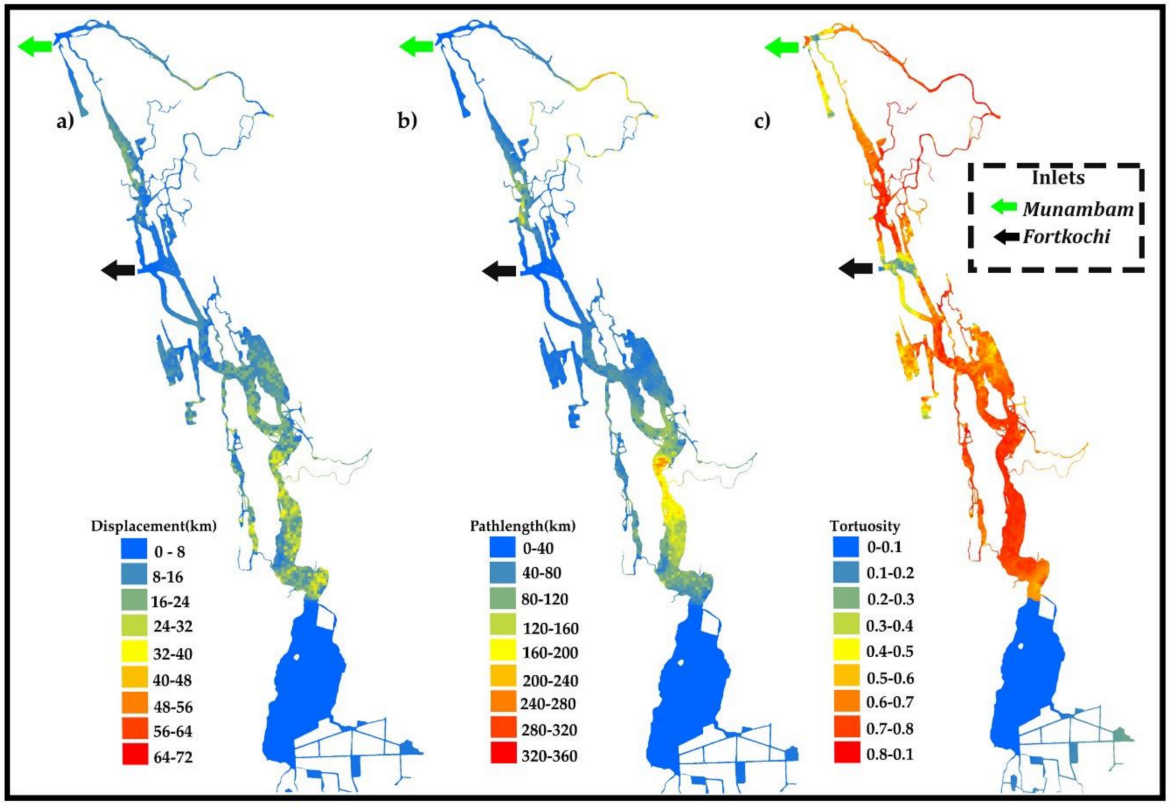

Figure 19. Displacement (**a**), path length (**b**) and tortuosity (**c**) of the CE during the control run simulation with Case 2 (river OFF and tide ON condition).

3.4. Comparison with World Wide Studies on Residence Time

Data collected from the 39 estuaries in the world was compared with river discharge, tidal length and residence time of the CE (Figure 20). A drastic variation in river discharge was noticed among these estuaries that varied from 0 to >10,000 m^3/s. These estuaries were categorised according to tidal amplitude, such as micro (0 to 2 m), meso (2 to 4 m) and macro (>4 m). Tidal length varied from 5 to >300 km and residence time spanned from 0 to 250 days. Normally estuaries with longer (smaller) tidal length have longer (smaller) residence time, but this residence time can be modified according to the river discharge. Estuaries like Chesapeake bay, N. San Francisco Bay, Delaware, Hudson, and Godavari belong to the micro tidal group, with an average freshwater influx of >300 m^3/s. Generally, microtidal estuaries exhibit longer residence time unless and until a high discharge that is comparable with the estuarine volume. Figure 20 infers that microtidal estuaries show longer residence time compared to meso and macrotidal estuaries. However, the river influx to these estuaries is higher than that of micro and meso tidal estuaries, which may not be sufficient to flush out the estuarine waters against tidal forcing. Hence, longer residence time can be attributed to the geometry (area and depth) and the ratio of freshwater volume to the total volume of the estuary. Among the microtidal estuaries, the tidal length of N. San Francisco Bay, Delaware, Hudson, Potomac and Hooghly estuaries are approximately twice that found in the Cochin estuary (47 km). On the contrary, residence time of these estuaries

are significantly less than the residence time of the CE (90 days). This could be attributed to the meandering of the CE and dual opening to the Arabian Sea.

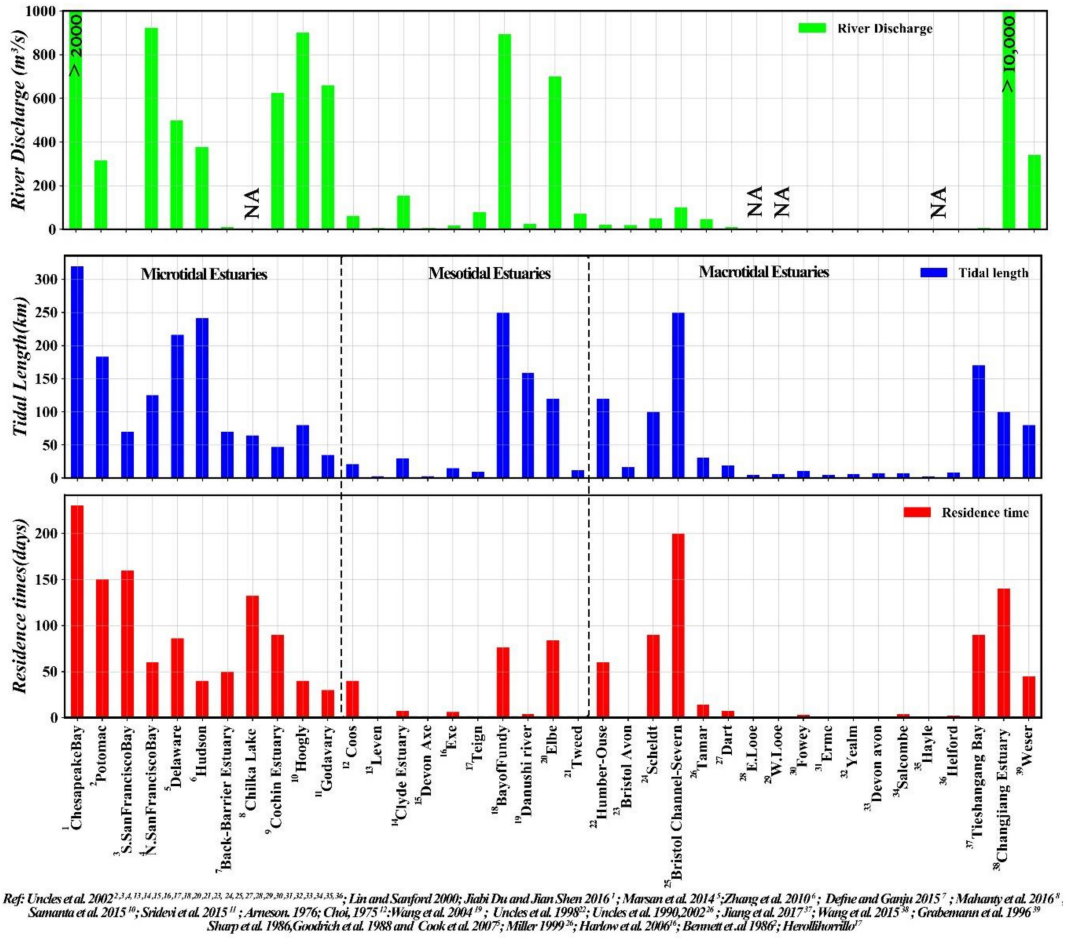

Ref: Uncles et al. 2002[2,3,4,13,14,15,16,17,18,20,21,23, 24,25,27,28,29,30,31,32,33,34,35,36]; Lin and Sanford 2000; Jiabi Du and Jian Shen 2016[1]; Marsan et al. 2014[5]; Zhang et al. 2010[6]; Defne and Ganju 2015[7]; Mahanty et al. 2016[8]; Samanta et al. 2015[10]; Sridevi et al. 2015[11]; Arneson. 1976; Choi, 1975[12]; Wang et al. 2004[19]; Uncles et al. 1998[22]; Uncles et al. 1990,2002[26]; Jiang et al. 2017[37]; Wang et al. 2015[38]; Grabemann et al. 1996[39]; Sharp et al. 1986, Goodrich et al. 1988 and Cook et al. 2007[9]; Miller 1999[26]; Harlow et al. 2006[16]; Bennett et al. 1986[9]; Herollihorrillo[17]

Figure 20. Comparison of residence time, tidal length and mean river discharge of the various estuaries in the world [30,32–50]. NA in the graph corresponds to "not available" discharge data, and two of the estuarine river discharges exceed more than 1000 m^3/s, therefore the values are marked in the plot (>2000 m^3/s and >10,000 m^3/s).

3.5. Pollution Transport Mechanism with Special Emphasis to the Tortuosity and Residence Time

Spatio-temporal variations of the particles during their transport from source to flush-out point undergo various processes such as diffusion, dispersion, settling or resuspension. These processes are linked with tortuosity and can be a proxy to the active and passive nature of the system. Irrespective of the season, estuarine regions near to the inlets (≤8 km) were found to be fast flushing zones (<1 day), with an average tortuosity of 0.3. Even though large freshwater influx is received by the CE during the monsoon, residence time (Table 5) showed significant spatial variations from 2.5 to 25 days (Figure 21). Congruently, a drastic increase in the tortuosity and residence time (Table 5) was noticed from monsoon to pre-monsoon (Figure 22) in the CE except 8 km near the inlet regions. The residence time of station 1 was increased from 4 days in monsoon (path length of 20 km) to 23 days (path length of 70 km) in pre-monsoon. The particle displacement at station 5 was negligibly small during monsoon and pre-monsoon though it registered a high tortuosity (≥0.7). Particles released in this region were retained for a longer period, covering pre-monsoon and monsoon with a path length of 43–45 km. This could be due to the opposing tidal propagation through this region from the two inlets. The stagnant nature of this region was noticed earlier by Balachandran et al. (2005 and 2006) as high accumulation of pollutants in the water column and sediment throughout the season.

Studies by Kumar et al. (2011) [51], Anas et al. (2015) [52] and Sheeba et al. (2017) [53] revealed that the contamination of heavy metal concentration in the water was higher during the pre-monsoon than monsoon at station 1. Tortuosity values were high during pre-monsoon, which supports the process of precipitation, co-precipitation and flocculation of metals [10,11,13,54]. The maximum path length of 350 km (10-fold longer than the actual axial distance from the inlet) observed at station 15 (Figure 16a,b and 22h) during the pre-monsoon could be attributed to the amplification of tidal currents due to the funnelling effect, which favours the retention capacity of pollutants or holds degraded water in the system for a long time. However, during the monsoon, this region exhibited a reduced path length of 120 km (Figure 13a, b and 21h) (3-fold longer than the actual axial distance from the inlet) and shorter residence time (7.5 days). In general, upstream of the CE exhibited longer residence time during the pre-monsoon (180 flood-ebb cycles) and minimum during monsoon (50 flood-ebb cycles), which was well justified with tortuosity values (Table 5).

During the closure period of Thanneermukkom barrage (pre-monsoon), the barrage prevents natural flushing and enhances tidal amplification [55,56], resulting in a negligible displacement (Figure 15b–d) due to the generation of the standing wave. This could modify the prevailing dynamics and resulted in a stagnant water body about 8 km north of the barrage with tortuosity of 0.7, while south of the barrage exhibited with least path length, tortuosity and longer residence time due to the interruption of the natural ebb-flood flow (Figure 22i). Negligible flushing with shorter path length and a heavy load of pollutants such as pesticides and fertilizers to this region from the paddy fields promotes the proliferation of weeds and water hyacinths. Annually, 180,000 tourists visit the southern estuary [18,57] and many of them utilize houseboats (~604 houseboats) for recreational purposes that increase the dumping of effluents, oil and solid waste to the system. These activities can enhance the accumulation of pollutants/material to the sediment layers due to the stagnant nature of the water body during the barrage closure period. A serious concern is needed to prevent the accumulation of pollutants in the vicinities of the Thanneermukkom barrage. The study highlights a drastic drop in the flushing efficiency with a larger path length during the low discharge period to an increased flushing nature by high riverine influx during the high river discharge period. Longer residence time noticed in the CE during the pre-monsoon could be due to the generation of higher tidal harmonics, geomorphologic alteration, increased residual circulations and reduced river discharge. These factors result in an oscillating water body and enhance accumulation of pollutants in the estuarine environment. These finding underlines ameliorative management of wastewater discharge from the point and non-point sources to the CE. Estuarine livelihoods, such as agriculture, fishing, transport and tourism, are likely to be enhanced by a more rational and optimum utilization of the the integral knowledge of site-specific transport trajectories and residence times.

Table 5. Comparison of residence time, path length, tortuosity at various locations in the monsoon and pre-monsoon periods.

Sl. No	Locations	Residence Time		Path Length		Tortuosity		Flushing Inlet
		Monsoon	Pre-Monsoon	Monsoon	Pre-Monsoon	Monsoon	Pre-Monsoon	
a	Cherai	2.6	10	20	30	0.4	0.5	Munambam
b	Nedungad	25	90	45	43	0.70	0.73	Munambam
c	Periyar	4	23	20	70	0.34	0.76	Fortkochi
d	Thevara	4	15	22	52	0.53	0.75	Fortkochi
e	Arookutty	5	20	50	74	0.55	0.63	Fortkochi
f	Murinjapuzha	6.6	90	90	130	0.57	0.75	Fortkochi
g	Makayilkadavu	7.5	90	120	350	0.68	0.89	Fortkochi
h	Thanneermukkom	17.5	90	130	63	0.70	0.72	Fortkochi
i	Alappuzha	21	90	160	3	0.70	0.03	Fortkochi

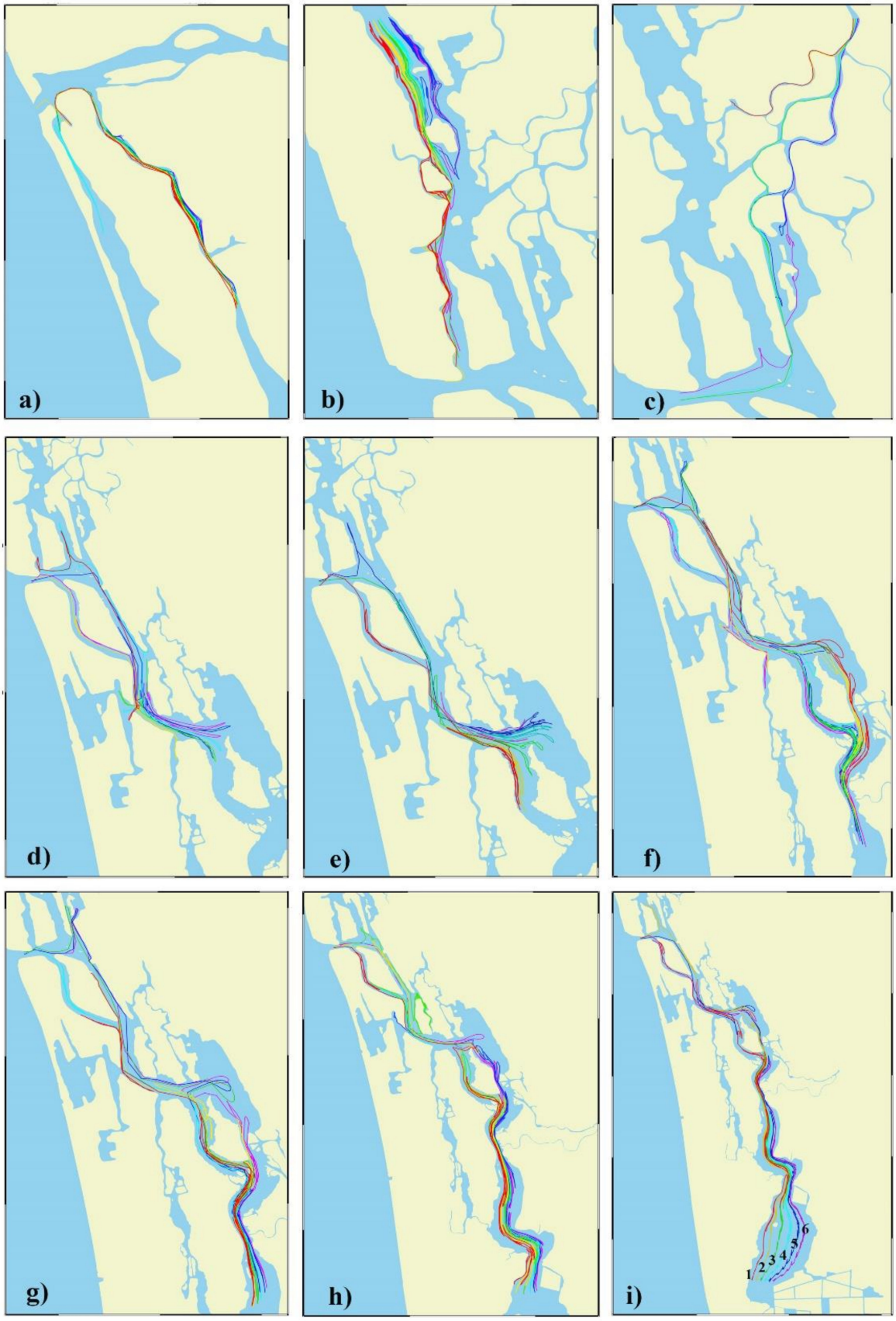

Figure 21. Trajectories of the particles released at nine locations as mentioned in the Table 5 (**a**–**i**) during the monsoon period is shown as Red (1), yellow (2), green (3), cyan (4), blue (5) and magenta (6) according to its lateral position.

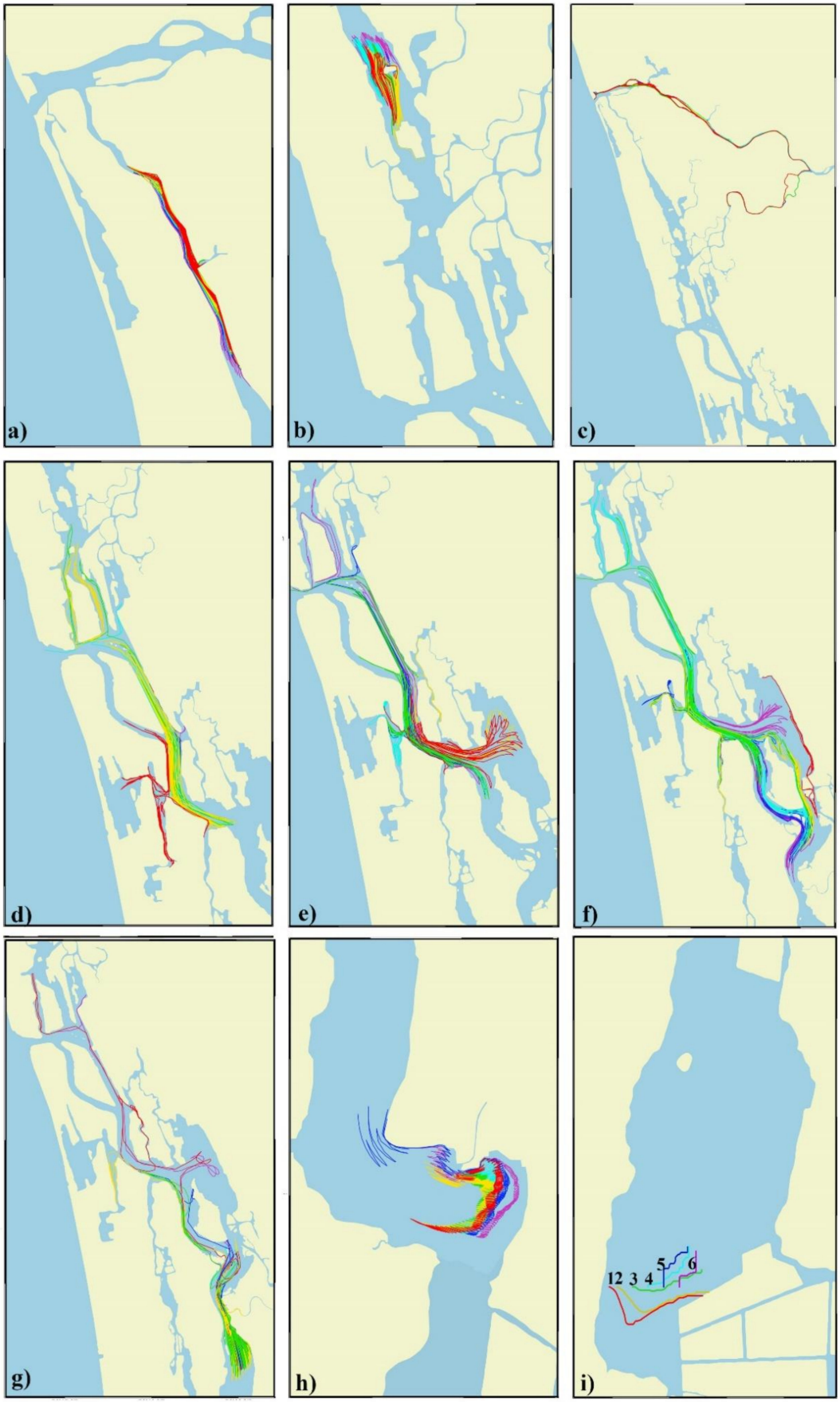

Figure 22. Trajectories of the particles released at nine locations as mentioned in the Table 5 (**a**–**i**) during the pre-monsoon period is shown as Red (1), yellow (2), green (3), cyan (4), blue (5) and magenta (6) according to its lateral position.

4. Conclusions

A thorough understanding of the pollutant transport and dispersal mechanism in estuaries are highly essential for their sustainable management. Cochin city is one of the densely populated regions in India, where most of the industries in the state are co-located. Hence an understanding of the hydrodynamic behavior, its mixing and flushing time scales, is highly essential to the legislation of policymakers to implement sustainable management of the estuary. A hydrodynamic model (FVCOM) coupled with a particle tracking module was used to study pollution transport trajectories and its residence times with respect to seasonal river discharge. Spatio-temporal patterns of the particle distribution in the CE showed similar trends during the monsoon and post-monsoon with an average residence time of 25 and 30 days, respectively. The longer residence time of 90 days noticed during the pre-monsoon could be attributed to low river discharge and tidal incursion to the upstream regions, eventually resulting in limited transport. This augments the retention capacity of pollutants in the system for a long time with longer path lengths and high tortuosity. Shorter path length, tortuosity and shorter residence during the monsoon significantly modified the flushing efficiency of the CE. Irrespective of the season, estuarine regions nearer to the inlets of Fortkochi and Munambam were found to be fast flushing zones with minimum tortuosity. Slow flushing zones were demarcated at Nedungad (all seasons) and Thanneermukkom (pre-monsoon). The sluggish movement noticed in the Nedungad region was due to the opposing tidal forces entering from two inlets, whereas during the closure of the Thanneermukkom barrage, tidal wave reflect from the barrage results in a standing wave.

The experiments carried out tide OFF and river ON (Case 1) are almost similar to the monsoon condition of the CE, while tide ON and river OFF (Case 2) typically simulated the pre-monsoon scenario. This confirms that seasonal forcing has a significant influence on the flushing characteristics and residence time of the CE. Thus, the major factor that controls the flushing characteristics and residence time of the Cochin estuary is river discharge during the monsoon, while that of the pre-monsoon is driven by tidal dynamics and geomorphological settings. Since the CE experiences untreated pollution stress from all directions, stringent measures must be adopted before any catastrophic events affect this estuary. These results emphasise the need for proper treatment of pollutants before they are released into the estuary, especially during the pre-monsoon period due to the longer residence time. This is crucial information for multiple stakeholders in the planning and adaptive management of developmental activities in the CE that supports a healthy and sustainable estuarine environment.

Supplementary Materials: The following are available online at http://www.mdpi.com/2073-4441/12/3/908/s1, Video S1: Particle tracking animation during the monsoon and pre-monsoon, Video S2: An animation of salinity changes with respect to ebb-flood periods during high discharge period, Figure S1: Bathymetry of the Model domain with 10-uniform sigma layers, Figure S2: Bathymetry map of the model domain overlaid with Landsat -8 Satellite image, Figure S3: Validation of surface water elevation during the pre-monsoon period (2010-2-22 to 2010-03-21), Figure S4: Validation of surface water elevation during the monsoon period (2010-07-25 to 2010-08-21), Figure S5a: Validation of along channel velocity and across channel velocity during the pre-monsoon period (2010-2-22 to 2010-03-21), Figure S5b. Validation of along channel velocity and across channel velocity during the pre-monsoon period (2010-2-22 to 2010-03-21), Figure S6a: Validation of along channel velocity and across channel during the monsoon period (2010-07-25 to 2010-08-21), Figure S6b: Validation of along channel velocity and across channel during the monsoon period (2010-07-25 to 2010-08-21), Figure S7a: Validation of along flow velocity and flow direction during the pre-monsoon period (2010-2-22 to 2010-03-21), Figure S7b: Validation of along flow velocity and flow direction during the pre-monsoon period (2010-2-22 to 2010-03-21), Figure S8a: Validation of along flow velocity and flow direction during the monsoon period (2010-07-25 to 2010-08-21), Figure S8b: Validation of along flow velocity and flow direction during the monsoon period (2010-07-25 to 2010-08-21), Figure S9: Validation of salinity below surface (0.4 m depth) at six locations during 2013-2014. Figure S10a: FVCOM Model Surface salinity at flood period 2014-04-02 13:30 (pre-monsoon), Figure S10a: FVCOM Model Surface salinity at flood period 2014-04-02 13:30 (pre-monsoon), Figure S10b: FVCOM Model Surface salinity at ebb period 2014-04-03 6:29 (pre-monsoon), Figure S11a: FVCOM Model Surface salinity at flood period 2014-07-06 13:30 (monsoon), Figure S11b: FVCOM Model Surface salinity at flood period 2014-07-14 13:30 (monsoon), Figure S12: Model comparison of the particle transport with float experiment at Fortkochi during the 10th March 2016.

Author Contributions: Conceptualization, S.J. and K.R.M.; Formal analysis, G.S.; Investigation, S.J. and K.R.M.; Methodology, S.J., S.A.A., G.S. and P.W.C.; Software, S.A.A. and K.R.M.; Supervision, K.R.M. and C.R.; Validation, S.J. and C.R.; Visualization, S.J. and S.A.A.; Writing—original draft, S.J.; Writing—review & editing, K.R.M., C.R., S.A.A. and G.S. All authors have read and agreed to the published version of the manuscript.

Funding: This study was partially funded by Naval Research Board (GAP3168) and Council of Scientific & Industrial Research, India (PSC0105).

Acknowledgments: The authors thank Director, NIO, Goa, and Scientist-in-Charge, NIO, Cochin, for the encouragement and support. We are grateful to A.C. Anil, Project Leader, OCEAN FINDER (PSC 0105) for financial support. We acknowledge ICMAM, Chennai (Ministry of Earth Sciences, India), Naval Research Board (NRB) and CSIR-NIO (Council of Scientific & Industrial Research, India) for the financial support to carry out this study. We wish to record a special thanks to Athul Rajeev for the technical support. Fifth author, Seena G. acknowledge Department of Science and Technology, India for the financial support under WOS-A scheme (GAP 2908). We want to thank the FVCOM development team members in the Marine Ecosystem Dynamics and Modeling Laboratory, School of Marine Science and Technology, UMASSD for providing FVCOM source code. This is CSIR-NIO contribution No. 6499

Conflicts of Interest: The authors declare no conflict of interest.

References

1. Liu, W.X.; Li, X.D.; Shen, Z.G.; Wang, D.C.; Wai, O.W.H.; Li, Y.S. Multivariate statistical study of heavy metal enrichment in sediments of the Pearl River Estuary. *Environ. Pollut.* **2003**, *121*, 377–388. [CrossRef]
2. Lancelot, C.; Billen, G. Activity of heterotrophic bacteria and its coupling to primary production during the spring phytoplankton bloom in the southern bight of the North Sea. *Limnol. Oceanogr.* **1984**, *29*, 721–730. [CrossRef]
3. Monsen, N.E.; Cloern, J.E.; Lucas, L.V.; Monismith, S.G. A comment on the use of flushing time, residence time, and age as transport time scales. *Limnol. Oceanogr.* **2002**, *47*, 1545–1553. [CrossRef]
4. Delhez, E.J.M.; Campin, J.-M.; Hirst, A.C.; Deleersnijder, E. Toward a general theory of the age in ocean modelling. *Ocean Model.* **1999**, *1*, 17–27. [CrossRef]
5. González, F.U.T.; Herrera-Silveira, J.A.; Aguirre-Macedo, M.L. Water quality variability and eutrophic trends in karstic tropical coastal lagoons of the Yucatán Peninsula. *Estuar. Coast. Shelf Sci.* **2008**, *76*, 418–430. [CrossRef]
6. Bolin, B.; Rodhe, H. A note on the concepts of age distribution and transit time in natural reservoirs. *Tellus* **1973**, *25*, 58–62. [CrossRef]
7. Takeoka, H. Fundamental concepts of exchange and transport time scales in a coastal sea. *Cont. Shelf Res.* **1984**, *3*, 311–326. [CrossRef]
8. Zimmerman, J.T.F. Mixing and flushing of tidal embayments in the western Dutch Wadden Sea part I: Distribution of salinity and calculation of mixing time scales. *Neth. J. Sea Res.* **1976**, *10*, 149–191. [CrossRef]
9. *Coastal Pollution Control Series: Central Pollution Control Board Report*; CPCB Pollution Potential of Industries in Coastal Areas of India; CPCB: New Delhi, India, 1996.
10. Nair, S.M.; Balchand, A.N. Phosphate-Phosphorus (Ad-)Sorption Characteristics of Sediments from a Very High Productive Coastal Zone. *Toxicol. Environ. Chem.* **1993**, *39*, 81–95. [CrossRef]
11. Martin, G.D.; George, R.; Shaiju, P.; Muraleedharan, K.R.; Nair, S.M.; Chandramohanakumar, N. Toxic metals enrichment in the surficial sediments of a eutrophic tropical estuary (Cochin Backwaters, Southwest Coast of India). *Sci. World J.* **2012**. [CrossRef]
12. Nair, M.P.; Sujatha, C.H. Environmental geochemistry of core sediment in the Cochin Estuary (CE), India. *Res. J. Chem. Sci.* **2013**, *3*, 65–69.
13. Balachandran, K.; Raj, C.M.L.; Nair, M.; Joseph, T.; Sheeba, P.; Venugopal, P. Heavy metal accumulation in a flow restricted, tropical estuary. *Estuar. Coast. Shelf Sci.* **2005**, *65*, 361–370. [CrossRef]
14. Narayanan, N.C.; Venot, J.-P. Drivers of change in fragile environments: Challenges to governance in Indian wetlands. *Nat. Resour. Forum* **2009**, *33*, 320–333. [CrossRef]
15. Sruthy, S.; Ramasamy, E.V. Microplastic pollution in Vembanad Lake, Kerala, India: The first report of microplastics in lake and estuarine sediments in India. *Environ. Pollut.* **2017**, *222*, 315–322. [CrossRef] [PubMed]
16. *KSPCB Kerala State Pollution Control Board Action Plan for Greater Kochi Area*; KSPCB: Kerala, India, 2010.
17. Rajan, P.D.; Purushothaman, S.; Krishnan, S.; Kiran, M.C.; Deepak, D.; Jojo, T.D. Strengthening Communities and Institutions for Sustainable Management of Vembanad Backwaters, Kerala. In Proceedings of the Taal 2007: The 12th World Lake Conference, Jaipur, India, 28 October–2 November 2007; pp. 1158–1163.

18. Remani, K.N.; Jayakumar, P.; Jalaja, T.K. Environmental Problems and Management Aspects of Vembanad Kol Wetlands in South West Coast of India. *Nat. Environ. Pollut. Technol.* **2010**, *9*, 247–254.
19. Lallu, K.R.; Fausia, K.H.; Vinita, J.; Balachandran, K.K.; Naveen Kumar, K.R.; Rehitha, T.V. Transport of dissolved nutrients and chlorophyll a in a tropical estuary, southwest coast of India. *Environ. Monit. Assess.* **2014**, *186*, 4829–4839. [CrossRef]
20. Janardanan, V.; Amaravayal, S.; Revichandran, C.; Manoj, N.T.; Muraleedharan, K.R.; Jacob, B. Salinity Response to Seasonal Runoff in a Complex Estuarine System (Cochin Estuary, West Coast of India). *J. Coast. Res.* **2015**, *31*, 869–878. [CrossRef]
21. Chen, C.; Liu, H.; Beardsley, R.C. An unstructured grid, finite-volume, three-dimensional, primitive equations ocean model: Application to coastal ocean and estuaries. *J. Atmos. Ocean. Technol.* **2003**, *20*, 159–186. [CrossRef]
22. Srinivas, K.; Revichandran, C.; Thottam, T.J.; Maheswaran, P.A.; Mohamed Asharaf, T.T.; Murukesh, N. Currents in the Cochin estuarine system [southwest coast of India] during March 2000. *Indian J. Mar. Sci.* **2003**, *32*, 123–132.
23. Revichandran, C.; Srinivas, K.; Muraleedharan, K.R.; Rafeeq, M.; Amaravayal, S.; Vijayakumar, K.; Jayalakshmy, K.V. Environmental set-up and tidal propagation in a tropical estuary with dual connection to the sea (SW Coast of India). *Environ. Earth Sci.* **2012**, *66*, 1031–1042. [CrossRef]
24. Shivaprasad, A.; Vinita, J.; Revichandran, C.; Manoj, N.T.; Jayalakshmy, K.V.; Muraleedharan, K.R. Ambiguities in the classification of Cochin estuary, West coast of India. *Hydrol. Earth Syst. Sci. Discuss.* **2013**, *10*, 3595–3628. [CrossRef]
25. Geuzaine, C.; Remacle, J.-F. Gmsh: A 3-D finite element mesh generator with built-in pre-and post-processing facilities. *Int. J. Numer. Methods Eng.* **2009**, *79*, 1309–1331. [CrossRef]
26. Willmott, C.J. On the validation of models. *Phys. Geogr.* **1981**, *2*, 184–194. [CrossRef]
27. Churchill, J.H.; Runge, J.; Chen, C. Processes controlling retention of spring-spawned Atlantic cod (Gadus morhua) in the western Gulf of Maine and their relationship to an index of recruitment success. *Fish. Oceanogr.* **2011**, *20*, 32–46. [CrossRef]
28. Huret, M.; Runge, J.A.; Chen, C.; Cowles, G.; Xu, Q.; Pringle, J.M. Dispersal modeling of fish early life stages: Sensitivity with application to Atlantic cod in the western Gulf of Maine. *Mar. Ecol. Prog. Ser.* **2007**, *347*, 261–274. [CrossRef]
29. Anderson, E.J.; Phanikumar, M.S. Surface storage dynamics in large rivers: Comparing three-dimensional particle transport, one-dimensional fractional derivative, and multirate transient storage models. *Water Resour. Res.* **2011**, *47*. [CrossRef]
30. Defne, Z.; Ganju, N.K. Quantifying the residence time and flushing characteristics of a shallow, back-barrier estuary: Application of hydrodynamic and particle tracking models. *Estuaries Coasts* **2015**, *38*, 1719–1734. [CrossRef]
31. Ramamirtham, C.P.; Muthusamy, S. Estuarine oceanography of the Vembanad lake Part II: The region between Cochin and Azhikode. *Indian J. Fish.* **1986**, *33*, 218–224.
32. Du, J.; Shen, J. Water residence time in Chesapeake Bay for 1980–2012. *J. Mar. Syst.* **2016**, *164*, 101–111. [CrossRef]
33. Uncles, R.J.; Stephens, J.A.; Smith, R.E. The dependence of estuarine turbidity on tidal intrusion length, tidal range and residence time. *Cont. Shelf Res.* **2002**, *22*, 1835–1856. [CrossRef]
34. Marsan, D.; Rigaud, S.; Church, T. Natural radionuclides 210Po and 210Pb in the Delaware and Chesapeake Estuaries: Modeling scavenging rates and residence times. *J. Environ. Radioact.* **2014**, *138*, 447–455. [CrossRef] [PubMed]
35. Zhang, W.G.; Wilkin, J.L.; Schofield, O.M.E. Simulation of water age and residence time in New York Bight. *J. Phys. Oceanogr.* **2010**, *40*, 965–982. [CrossRef]
36. Mahanty, M.M.; Mohanty, P.K.; Pattnaik, A.K.; Panda, U.S.; Pradhan, S.; Samal, R.N. Hydrodynamics, temperature/salinity variability and residence time in the Chilika lagoon during dry and wet period: Measurement and modeling. *Cont. Shelf Res.* **2016**, *125*, 28–43. [CrossRef]
37. Samanta, S.; Dalai, T.K.; Pattanaik, J.K.; Rai, S.K.; Mazumdar, A. Dissolved inorganic carbon (DIC) and its $δ$13C in the Ganga (Hooghly) River estuary, India: Evidence of DIC generation via organic carbon degradation and carbonate dissolution. *Geochim. Cosmochim. Acta* **2015**, *165*, 226–248. [CrossRef]

38. Sridevi, B.; Sarma, V.; Murty, T.V.R.; Sadhuram, Y.; Reddy, N.P.C.; Vijayakumar, K.; Raju, N.S.N.; Kumar, C.H.J.; Raju, Y.S.N.; Luis, R.; et al. Variability in stratification and flushing times of the Gautami–Godavari estuary, India. *J. Earth Syst. Sci.* **2015**, *124*, 993–1003. [CrossRef]
39. Arneson, R.J. Seasonal Variations in Tidal Dynamics, Water Quality, and Sediments in the Coos Bay Estaury. Master's Thesis, Oregon State University, Corvallis, OR, USA, 1975.
40. Choi, B. Pollution and Tidal Flushing Predictions for Oregon's Estuaries. Master's Thesis, Oregon State University, Corvallis, OR, USA, 1975.
41. Wang, C.-F.; Hsu, M.-H.; Kuo, A.Y. Residence time of the Danshuei River estuary, Taiwan. *Estuar. Coast. Shelf Sci.* **2004**, *60*, 381–393. [CrossRef]
42. Jiang, C.; Liu, Y.; Long, Y.; Wu, C. Estimation of Residence Time and Transport Trajectory in Tieshangang Bay, China. *Water* **2017**, *9*, 321. [CrossRef]
43. Wang, Y.; Shen, J.; He, Q.; Zhu, L.; Zhang, D. Seasonal variations of transport time of freshwater exchanges between Changjiang Estuary and its adjacent regions. *Estuar. Coast. Shelf Sci.* **2015**, *157*, 109–119. [CrossRef]
44. Grabemann, I.; Kühle, H.; Kunze, B.; Müller, A. Studies on transport times and water quality in the Weser estuary (Germany). *Coast. Estuar. Stud.* **1996**, *50*, 291–301.
45. Cook, T.L.; Sommerfield, C.K.; Wong, K.-C. Observations of tidal and springtime sediment transport in the upper Delaware Estuary. *Estuar. Coast. Shelf Sci.* **2007**, *72*, 235–246. [CrossRef]
46. Sharp, J.H.; Cifuentes, L.A.; Coffin, R.B.; Pennock, J.R.; Wong, K.-C. The influence of river variability on the circulation, chemistry, and microbiology of the Delaware Estuary. *Estuaries* **1986**, *9*, 261–269. [CrossRef]
47. Miller, A.E.J. Seasonal investigations of dissolved organic carbon dynamics in the Tamar Estuary, UK. *Estuar. Coast. Shelf Sci.* **1999**, *49*, 891–908. [CrossRef]
48. Harlow, A.; Webb, B.; Walling, D. Sediment yields in the Exe Basin: A longer-term perspective. *IAHS Publ.* **2006**, *306*, 12.
49. Bennett, J.P.; Woodward, J.W.; Shultz, D.J. Effect of discharge on the chlorophylla distribution in the tidally-influenced Potomac River. *Estuaries* **1986**, *9*, 250–260. [CrossRef]
50. Herollihorrillo-Caraballo, J.; Reeve, D.; Simmons, D.; Pan, S. *Present and Future Conditions from Plymouth Sound to Exe Estuary*; University of Plymouth: Plymouth, UK, 2011.
51. Kumar, A.A.; Dipu, S.; Sobha, V. Seasonal variation of heavy metals in cochin estuary and adjoining Periyar and Muvattupuzha rivers, Kerala, India. *Glob. J. Environ. Res.* **2011**, *5*, 15–20.
52. Anas, A.; Jasmin, C.; Sheeba, V.A.; Gireeshkumar, T.R.; Nair, S. Heavy metals pollution influence the community structure of Cyanobacteria in nutrient rich tropical estuary. *Digit. Repos. Serv.* **2015**. [CrossRef]
53. Sheeba, V.A.; Abdulaziz, A.; Gireeshkumar, T.R.; Ram, A.; Rakesh, P.S.; Jasmin, C.; Parameswaran, P.S. Role of heavy metals in structuring the microbial community associated with particulate matter in a tropical estuary. *Environ. Pollut.* **2017**, *231*, 589–600. [CrossRef]
54. Nair, S.M.; Balchand, A.N.; Nambisan, P.N.K. Metal concentrations in recently deposited sediments of Cochin backwaters, India. *Sci. Total Environ.* **1990**, *97*, 507–524. [CrossRef]
55. Kumar, P.K.D.; Srinivas, K.; Muraleedharan, K.R.; Thottam, T.J. Observed mixed standing-wave signatures in Cochin Estuary on the southwest coast of India. *J. Coast. Res.* **2009**, *25*, 1106–1113. [CrossRef]
56. Shivaprasad, A.; Vinita, J.; Revichandran, C.; Manoj, N.T.; Srinivas, K.; Reny, P.D.; Ashwini, R.; Muraleedharan, K.R. Influence of Saltwater Barrage on Tides, Salinity, and Chlorophyll a in Cochin Estuary, India. *J. Coast. Res.* **2013**, *29*, 1382–1390.
57. Chandy, J.; Raghunathan, R. Impact of Back Water Tourism in Kerala. *Int. J. Adv. Eng. Res. Dev.* **2017**, *4*, 227–232.